BRAIN TUMOR SEGMENTATION AND CLASSIFICATION USING MACHINE LEARNING

2023
MASTER THESIS
COMPUTER ENGINEERING

Ruaa Mashkoor MAHMOOD

Thesis Advisor
Assist. Prof. Dr. NEHAD T.A RAMAHA

BRAIN TUMOR SEGMENTATION AND CLASSIFICATION USING MACHINE LEARNING

Ruaa Mashkoor MAHMOOD

Thesis Advisor

Assist. Prof. Dr. NEHAD T.A RAMAHA

T.C.
Karabuk University
Institute of Graduate Programs
Department of Computer Engineering
Master Thesis
Prepared as

KARABUK
February 2023

I certify that in my opinion the thesis submitted by Ruaa Mashkoor MAHMOOD titled "EFFECTIVE BRAIN TUMOR SEGMENTATION AND CLASSIFICATION USING MACHINE LEARNING" is fully adequate in scope and in quality as a thesis for the degree of Master of Science.

Assist. Prof. Dr. NEHAD T.A RAMAHA .....
Thesis Advisor, Department of Computer Engineering

This thesis is accepted by the examining committee with a unanimous vote in the Department of Computer Engineering as a Master of Science thesis. February 27, 2023

Examining Committee Members (Institutions)		Signature
Chairman	: Assist. Prof. Dr. Zafer ALBAYRAK (SUBU)	.....
Member	: Assist. Prof. Dr. Kürşat Mustafa KARAOĞLAN (KBU)	.....
Member	: Assist. Prof. Dr. Nehad T.A RAMAHA (KBU)	.....

The degree of Master of Science by the thesis submitted is approved by the Administrative Board of the Institute of Graduate Programs, Karabuk University.

Prof. Dr. Müslüm KUZU .....
Director of the Institute of Graduate Program

"I declare that all the information within this thesis has been gathered and presented in accordance with academic regulations and ethical principles and I have according to the requirements of these regulations and principles cited all those which do not originate in this work as well."

Ruaa Mashkoor MAHMOOD

ÖZET

Yüksek Lisans Tezi

MAKİNE ÖĞRENMESİ YOLUYLA BEYİN TÜMÖRÜ SEGMENTASYONU VE SINIFLANDIRMASI

Ruaa Mashkoor MAHMOOD

Karabük Üniversitesi
Lisansüstü Eğitim Enstitüsü
Bilgisayar Mühendisliği Bölümü

Tez Danışmanı:
Dr. Öğr. Üyesi Nehad T.A RAMAHA

Şubat 2023, 67 sayfa

Beyin tümörleri tedaviye başlamadan önce MRG ile sınıflandırılmaları mümkün olan aberrant dokular koleksiyonudur. MRG taramalarının kullanılmasıyla yapılan tümör segmentasyonunun ve sınıflandırmasının zorlayıcı ve önemli çabalar olduğu bilinmektedir. Ancak bu segmentasyon ve sınıflandırma teşhis, preoperatif planlama ve postoperatif değerlendirmelerde kullanılabilir. Makine öğrenmesi modellerinin ve diğer teknolojilerin geliştirilmesi radyologların malinensileri hastaları esip biçmeden tespit edebilmelerini sağlayacaktır. Bu tezde MRG kontrast pekiştirme ardından sınırları belirsiz kümeleme teknikleri ve eşik oluşturma ve morfolojik işlemler kullanılmıştır. Önerilen model iki adımdan oluşmaktadır: tümörlerin ekstrakte edilmesi ve ölçümlerinin yapılması (segmentasyon) ve sonra beyin tümörlerinin tanımlanması ve sınıflandırılması için makine öğrenmesinin kullanılması. Ön işleme, kafatasının şeritlerle işaretlenmesi ve tümör segmentasyonu beyin tümörünün tespiti ve ölçümünde (büyüklük ve form) kullanılan adımlardır. Belli bir süre sonra CNN.

eğitimi için kullanılan eğitim kalemlerinin büyük sayısı nedeniyle CNN aşırı uyum göstermeye başlar. Artık aktarımlı öğrenme yöntemini kullanan CNN kullanmamızın nedeni budur. Beyin MRG'lerinde görülen tümörleri (glioma veya meningioma) sınıflandırmak için CNN bazlı Relu mimarisi ve HOG ve LPB üzerinden alınan özelliklerin birleştirildiği SVM kullanılır. Yöntemlerin etkililiği presisyon, geri çağırma, F-ölçümü ve doğrulukla ölçülmüştür. Sonuçlar LBP ve HOG ve modifiye CNN ile kombine SVM doğruluğunun %98 olduğunu göstermiştir

Anahtar Sözcükler : Makine öğrenmesi, Tümör segmentasyonu, Sınıflandırma, Özellik ekstraksiyonu, Ölçümler, MRG görüntüsü .

Bilim Kodu : 92431

ABSTRACT

Master. Thesis

BRAIN TUMOR SEGMENTATION AND CLASSIFICATION USING MACHINE LEARNING

Ruaa Mashkoor MAHMOOD

Karabük University
Institute of Graduate Programs
Department of Computer Engineering

Thesis Advisor:
Assist. Prof. Dr. NEHAD T.A RAMAHA
February 2023, 67 pages

A brain tumor is a collection of aberrant tissues, which makes it possible to classify them using MRI before beginning therapy. Tumor segmentation and classification from brain MRI scans are well-known to be challenging and important endeavors. However, this segmentation and classification can be used in diagnostics, preoperative planning, and postoperative evaluations. Therefore, this segmentation and classification can be used in diagnostics, preoperative planning, and postoperative evaluations. The development of machine learning models and other technologies will let radiologists detect malignancies without having to cut into patients. This thesis used a combination of fuzzy clustering techniques with thresholding and morphological operations following MRI contrast enhancement. The suggested model has two steps: extracting and measuring tumors (segmentation) and then using machine learning to identify and classify brain tumors. Pre-processing, skull stripping, and tumor segmentation are the steps in detecting a brain tumor and measurement (size and form).

After a certain period, CNN gets overfitted because of the large number of training images used to train them. That is why we now have CNN that uses transfer learning. CNN-based Relu architecture and SVM with fused retrieved features via HOG and LPB are used to classify brain MRI tumors (glioma or meningioma). The methods' efficacy has been measured by precision, recall, F-measure, and accuracy. The results showed that the accuracy of SVM with combined LBP with HOG is 97%, and modified CNN of 98%.

Key Word **:** Machine Learning, Tumor Segmentation, Classification, Feature Extraction, Measurements, MRI Image.

Science Code : 92431

ACKNOWLEDGMENT

I would like to give thanks to my advisor, Assist. Prof. Dr. Nehad RAMAHA, for his great interest and assistance in preparation of this thesis.

We are grateful to Karabük University for providing its software and hardware infrastructure to realize the current study.

Last but not least, I would also like to give special thanks to my family; none of this would be possible without you.

CONTENTS

Page

Page

LIST OF FIGURES

Page

LIST OF TABLES

Page

SYMBOLS ABBREVITIONS INDEX

MRI	:	Magnetic Resonance Imaging
PCA	:	Principal Component Analysis
FNN	:	Feed-Forward Neural Network
KNN	:	K-Nearest Neighbor
RT	:	Ripple Transform
BFC	:	Bayesian Fuzzy Clustering
ROI	:	Region Of Interest
WPTE	:	Wavelet Packet Tallies Entropy
JOA	:	Jaya Optimization Algorithm
DAE	:	Auto Encoder
FCM	:	Fuzzy C-Means
DOPS	:	Darwinian Optimization of Particle Swarm
X-Ray	:	X-Ray Imaging
CT	:	Computed Tomography
PET	:	Positron Emission Tomography
TE	:	Transmission Interval
GM	:	Gray Matter
WM	:	White Matter
BSO	:	The Brain-Storming Optimization
PSNLM	:	Pre-Smooth Non-Local Means Filter
PVE	:	Partial Volume Impact
LDA	:	Linear Discriminant Analysis
SMO	:	Sequential Minimal Optimization
DPOS	:	Darwinian Optimization of Particle Swarm
CLAHE	:	Contrast Limited Adaptive Histogram Equalization
ML	:	Machine Learning
CAD	:	Computer-Assisted Diagnosis

HOG	:	Histogram Of Oriented Gradients
LBP	:	Local Binary Pattern

PART 1

INTRODUCTION

1.1. OVERVIEW

An aberrant mass tissue that has been developed due to the abnormal growth of cells is called a tumor. Malignancies are masses of tissue generated by the unregulated proliferation of aberrant cells. The brain is the master controller and regulator of the body, making it the essential organ [1]. However, in some cases, malignancies are formed in the brain. There is not yet a well-defined explanation for what causes brain cancer. Due to their position in the brain, which is the body's most essential organ, malignant brain tumors have a high fatality rate despite being very uncommon (just 2.0 percent of all documented malignancies in the globe) [2]. As a direct result of this, proper brain tumor segmentation at an early stage is very necessary in order to reduce the overall percentage of fatalities. Imaging with an MRI requires a lot of manual effort and a significant amount of time.

The numerous anatomical components of the human body may be shown via the use of image-processing methods. Simple imaging techniques make it difficult to see the abnormal architecture of the human brain. The use of magnetic resonance imaging technology allows for the differentiation and clarification of the neural architecture of the human brain [3]. It is necessary to begin by concentrating on background subtraction, color visualization of the brain tumor region, fragmentation, size measurements, and classification to minimize complexity and improve the segmentation and measurement techniques performance of tumor size, position, and shape vary [4]. This way is required in order to maximize segmentation and measurement performance. Following this step, morphological filtering may be used to remove any noise that was produced as a result of the segmentation process.

Using high-precision segmentation may also determine a tumor's benign or malignant nature [5].

1.2. CLINICAL BACKGROUND AND REVIEW

Digital health uses medical imaging techniques and equipment to capture pictures of different parts of a patient's body for analysis and treatment. Magnetic resonance imaging (MRI) is a method for seeing the brain, spinal cord, and other soft tissues, in three dimensions. Primarily, it illustrates human anatomy and physiology [5].

The brain's role as the body's master controller makes it one of the most crucial organs. Infections, strokes, and tumors are just a few of the many medical conditions that may lead to brain damage. A brain tumor is a mass of abnormally developing cells that may be either malignant or noncancerous. MRI is the most important test for diagnosing brain tumors (MRI). Medical image processing of MRI images has recently attracted attention [6] due to the need for efficient and objective analysis of massive data sets. Brain cancer detection and the automated classification of brain tissue using MRI scans are both important for studying and diagnosing human mental health. The most crucial part of an MRI image's medical imaging operations is segmentation, which separates and identifies its constituent parts so they may be processed individually.

This article summarizes brain tumors and the methods currently used to diagnose them. The physical foundations of MRI are also covered in this chapter. The dataset acquisition and application to conventional MRI are detailed. Although the primary goal of this thesis is to segment brain tumors, the created approaches will be used for the other segmentation challenge of brain damage [7] to demonstrate their capacity to segment a picture. Ischemic stroke statistics and lesions are briefly examined.

Principal Component Analysis (PCA) and a wavelet transform (D-DWT) in two dimensions may be used to determine what features of an image are most significant (PCA). They employed a Feed-forward Neural Network (FNN) and a K-Nearest Neighbor algorithm to sort the data (KNN) [8]. In order to develop a Ripple Transform (RT) model, Das et al. [9] fed features into a Least Squares Support Vector Machine

classifier. Tumors might be detected with the use of a fluid vector and T1-weighted images [10]. Tumor location was determined using diffusion coefficients and diffusion tensor imaging [11]. Despite the best efforts of brain tumor researchers, it is challenging to zero down on the optimal feature to eliminate. Selecting appropriate training and testing samples is particularly challenging [12,13]. One of the most original approaches to MR brain classification was created by Amin et al. [14]. A Gaussian filter was used to reduce noise, and then embedding, cyclic, contrast, and block appearance features were obtained for segmentation processing, all while using the cross-validation method for classification to extract the features of the brain images. The fuzzy clustering membership of the original image was included into the Markov random field function, as described by Chen et al. [15]. This approach is quite effective since it utilizes a hybrid technique along with segmented supporting data.

To identify brain tumors, Raja et al. [16] combined a auto-encoder with a Bayesian fuzzy clustering-based segmentation strategy. They used a non-local mean filter as a pre-processing step to reduce the overall amount of noise. The BFC (Bayesian fuzzy clustering) method was used for dividing up brain tumors. After the segments were separated, they were analyzed using information-theoretic metrics, the scattering transform (ST), and Wavelet packet tally entropy to extract useful characteristics (WPT). The Jaya Optimization Algorithm (JOA) was utilized, with a soft-max regression strategy, to classify the DAE scans of the brain tumor location (Auto Encoder). In order to execute their simulations, they used the BRATS 2015 database.

For the purpose of automating the segmentation and detection of brain tumors, Arunkumar et al. [17] proposed an ANN-based model. Preliminary detection of brain tumors using MR data was performed using the finest features with no human intervention. There are three potential enhancements to their method for dividing up brain tumors. As a first step, they used K-means clustering to categorize the areas of the district by grayscale, a standard method for grouping MR data at the time. Secondly, the right object was picked using ANN owing to the training method. By the time the brain tumor reached the mitotic stage, all of the characteristic tissues associated with it had been eliminated. It's possible that grayscale features of brain tumors might help doctors tell the difference between benign and malignant ones. The

SVM method's segmentation and brain identification results are assessed in light of their model. Their model has a 94.0% precision, 90.0% sensitivity, and 96.7% specificity.

Figure 1.1 demonstrates how the state-of-the-art works have all segmented the tumor within the brain rather than at the brain's periphery.

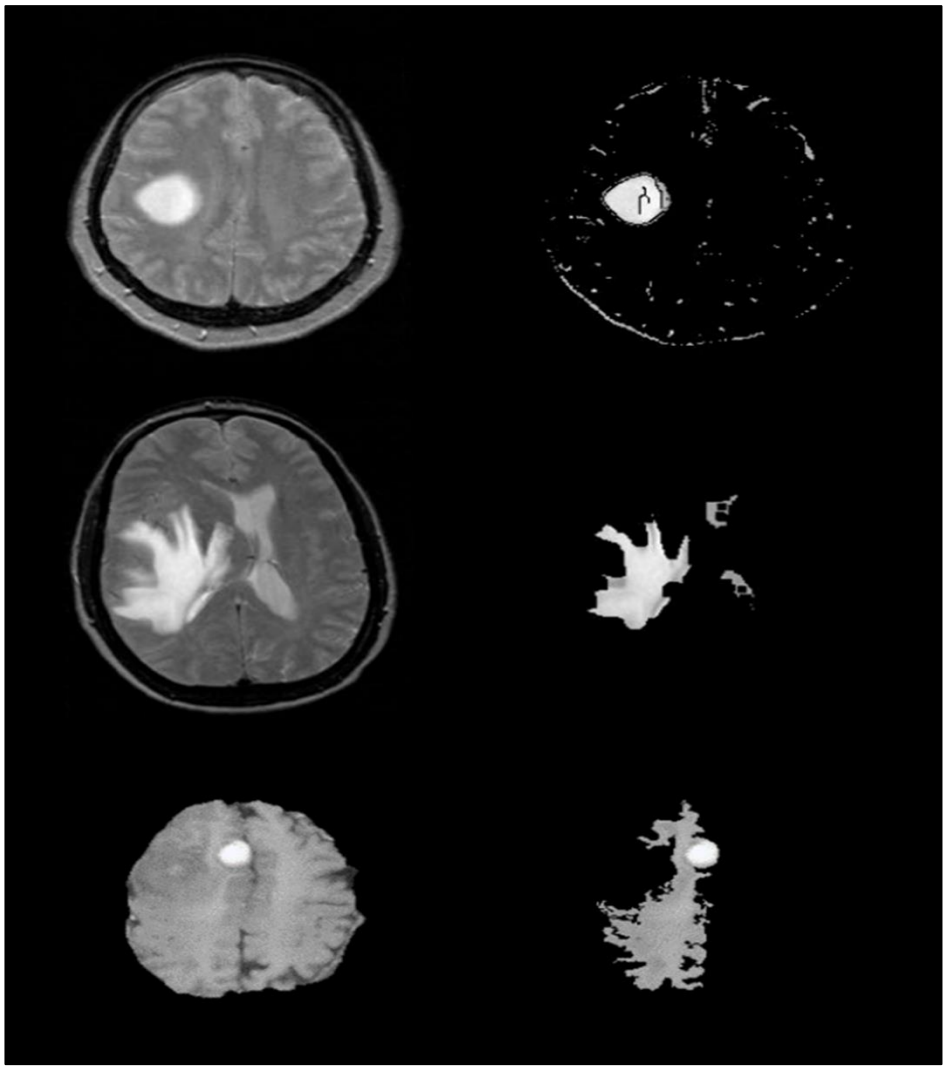

Figure 1.1. Examples of the different developed method

Mekhmoukh et al. [18] recommended using Particle Swarm Optimization (PSO) and rejecting outliers in conjunction with a level set. Segmenting brain tumors in an MR database is often done using the fuzzy c-means (FCM) method. This conventional method's membership function does not take into account contextual factors like

location. Depending on how the centroid is first set, the method is especially susceptible to image noise and unevenness. To improve the external suppression of standard FCM aggregation algorithms and reduce noise sensitivity, the authors created a new extended FCM picture segmentation approach. While the initial centers of clusters are selected at random in the FCM approach, the PSO algorithm selects centers of clusters based on their relevance to the problem at hand. Their program also considers topographical details in the immediate vicinity. In general, their strategy was successful.

The difficulty of the segmentation of a brain tumor is when the tumor is located at the boundary of the brain as an example in Figure 1.2 which is what our method will solve. One of the factors of the method that we research to develop is to solve the following difficulty, which is considered a research area for researchers and specialists.

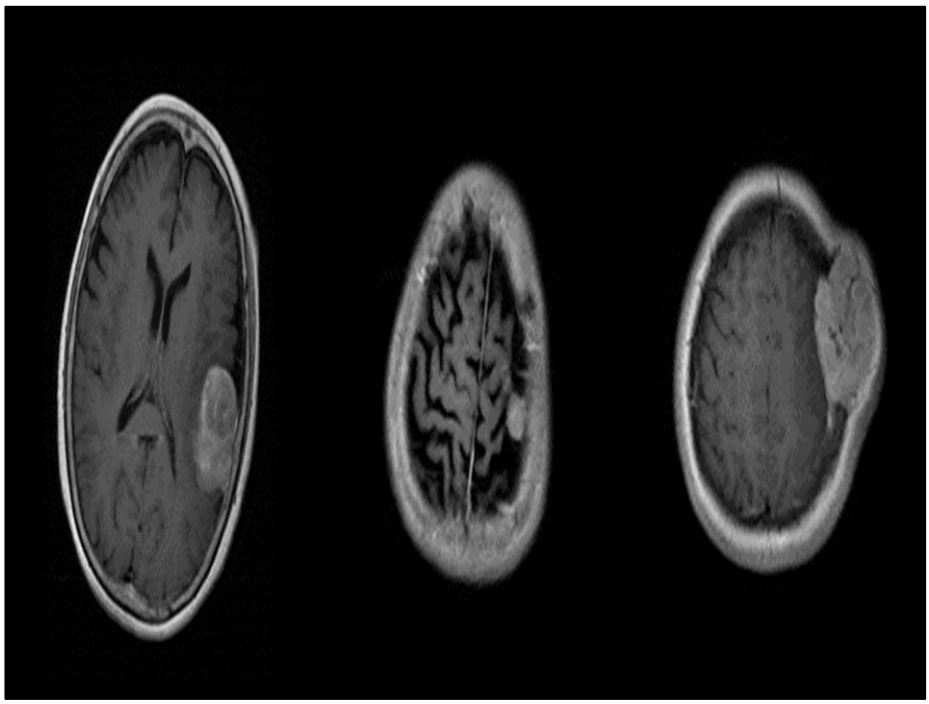

Figure 1.1. Example of difficult tumor segmentation located on the end of tumor

1.2. PROBLEM DEFINITION

In Europe, an estimated 60,000 people live with a brain tumor, with an additional 18,000 being diagnosed yearly. According to the NHS [1], the incidence of brain

tumors has increased in the United Kingdom, which is a serious concern. Aggressive gliomas account for about 82 percent of all brain and normal brain tumors [2]. This research highlights the need for a well-thought-out therapy for this kind of malignancy. Primary brain tumors are rare, although there are numerous brain tumors worldwide. Primary cancers that spread outside the brain and central nervous system are uncommon. On the other hand, the great majority of brain tumors are metastatic tumors that originate elsewhere in the body and spread to the brain through the bloodstream or lymphatic arteries.

The size, cell type, and stage of the tumor all have an impact on how well it responds to therapy. As a consequence, tumor segmentation is critical for surgical and other forms of therapeutic planning. Medical imaging methods may be used to identify and evaluate tumors. Choosing the best treatment for a variety of clinical conditions in order to support surgery and schedule radiation [4].

The whole 3D volume of the tumor must be accurately measured, which is accomplished by manually drawing a circle around the tumor's target region. Semi-automatic methods, on the other hand, take less time to segment each tumor. Because humans have a limited capacity to detect visible qualities in an image, manual segmentation is more prone to human errors. Accurate segmentation and identification will always be advantageous, especially when dealing with large MRI datasets.

- Our study involves time-consuming and automated brain tumor segmentation, measurements, and classification.
- Normally the anatomy of the brain is analyzed by MRI scans.
- Our system aims to detect the tumor from the given MRI scan and then measure the tumor size from the brain.
- The method is projected to enhance the present brain tumor screening technique and, by reducing the need for follow-up treatments, potentially lower healthcare expenses. Many processing stages are necessary for the appropriate characterization and interpretation of biological imaging data.

1.4. MOTIVATION

The human body has an astonishing number of cells. When a cell's growth becomes uncontrolled, it becomes a tumor. Imaging modalities such as CT and MRI scans are used to identify tumors. Using a range of technologies, such as medical image processing, machine learning, and computer vision, we seek to separate and label brain tumors in this study consistently. Neurosurgeons, radiologists, and other healthcare professionals may employ this procedure. MATLAB, an industry-standard simulation software tool, will be employed to improve the sensitivity, specificity, accuracy, and diagnostic efficiency of brain tumor screening. This way is expected to enhance current brain tumor screening approaches, possibly resulting in healthcare costs due to fewer follow-up scans. A multitude of processing techniques is required for the accurate classification and interpretation of biological imaging data.

This software is meant to aid doctors and radiologists in the early, cheap, and painless diagnosis of brain tumors. In medical image processing, computational methods are becoming more common. Medical decision-making, including risk assessment and disease categorization, relies heavily on tissue and organ segmentation. Research on segmentation has revealed useful information for analysis, diagnosis, and treatment planning. When diagnosing and planning therapy for brain tumors, proper segmentation may help since it provides a rapid and objective assessment of the tumor volume. Brain tumor segmentation is still a developing field after years of study.

1.5. AIM AND OBJECTIVES

The goal of this thesis is to create an automated image processing system for properly segmenting and classifying brain tumor and sub-tumor tissue from multimodal MR data, and time-consuming.

The following goals must be met in order to attain this goal:

- To explore feature representations for accurate brain tumor segmentation and size measurements that combine handmade features (which address local dependencies) with machine-learned features (which offer global information).
- To investigate the most efficient combination of features retrieved from multi-modal MR scans while maximizing the valuable information from specific MR modalities.
- To use a single, widely used MRI technique, develop an automated approach for generating a tumor segment that agrees with experts' delineation across all grades of glioma.
- To use machine learning for classification after extracting features from a segmented tumor and categorizing it.

1.6. ORGANIZATION OF THESIS

Five chapters make up the thesis work. This chapter introduces the notion of a brain tumor, the diagnostic of a brain tumor (segmentation, measurement, and cancer predication), and the procedures used to assess the brain. The problem statement and the thesis's goals are also presented in this section. The review of the literature presented in Chapter 2 is the focus of chapter 2, the latest and most relevant research is also included. The segmentation and classification techniques described in Chapter 3 are covered in great depth by the machine learning algorithms and computer vision approaches. For the evaluation of computer vision of segmentation technique and machine learning for cancer prediction, findings from experiments are presented in Chapter 4. Chapter 5 concluded the study with a summary of the findings and a list of suggestions for further research.

PART 2

LITERATURE REVIEW

2.1.CLASSIFICATION OF BRAIN TUMORS

The dissection and classification of brain tumors are both functions that are carried out by the nervous system of the human body. The hypothalamus is in charge of a variety of functions across the body, including cognition, movement, breathing, transmission, and heart rate [18–20]. Since tumors are defined by the proliferation of cancerous development, they have the potential to be a main cause of increased mortality in newborns as well as adults. Tumors may be found in or near the brain. Primary and secondary tumors are both eligible for analysis to determine whether they are benign or malignant [21].

Imaging techniques such as computed tomography (CT), magnetic resonance imaging (MRI), and x-ray imaging (X-Ray) may be used to analyze the anatomy of the brain and detect cancerous growths [22–24]. The use of magnetic resonance imaging (MRI) is becoming more widespread in the diagnosis of brain cancer [25–27]. The computer vision brain tumor segmentation technique uses this approach to split an image into parts by dividing the surrounding pixels of the picture into certain defined pixel attributes or qualities [28].

[Note: this method is also referred to as pixel separation]. In medical imaging, the major goal is to extract relevant information and correct object data with the lowest possible amount of error. This is one of the reasons why error correction is so important. The first thing that has to be done in medical image analysis is to get the picture ready to be processed. At this stage, the picture is prepared for the subsequent phase of post-processing by performing a variety of tasks, including filtering and noise removal [29]. The use of preprocessing software allows for the enhancement of images

for use in medical reasons. This may be accomplished by modifying the features of the picture in order to improve its visual qualities [30]. The second phase involves the implementation of separation operators as well as morphological operators. They are responsible for determining the size of the tumor as well as its location [31].

In the field of image processing, segmentation is a very crucial operation that plays a vital part in extracting information from complex medical scans. This information may be used to diagnose and treat patients. Image segmentation's primary objective is to break up a digital picture into distinct parts that cannot be combined with one another [32].

The process of segmenting an image may be carried out in a variety of different methods [33]. Two examples of segmentation methods are region-based segmentation and edge detection segmentation that makes use of clustering algorithms. After medical scans have been processed and segmented, feature extractions are necessary in order to differentiate cancers based on the specific intensity strength or texture pattern that they exhibit [34].

Radiologists classify brain tumors according to whether or not they have a homogeneous or heterogeneous texture [35]. This allows them to differentiate between the many types of cancer. These observable characteristics provide us with suggestions for how to develop a computer-aided diagnosis (CAD) that is able to determine whether or not a person has brain cancer [36].

2.2. TYPES OF MEDICAL IMAGES

[37] Some examples of medical images that use a variety of imaging techniques include computed tomography (CT), magnetic resonance imaging (MRI), and chest x-rays (CXR). Other examples of medical images that use a variety of imaging techniques include positron emission tomography (PET) and nuclear magnetic resonance imaging (NMR). However, owing to the massive number of data generated by this method, effective quantitative evaluations can only be used in clinical practice under very particular circumstances [38]. This is because this method generates such

a large amount of data. In most cases, computed tomography (CT) imaging is favored over magnetic resonance imaging (MRI) because to its wider availability, cheaper cost, and improved early-stock sensitivity. CT gives the facts essential to make accurate judgements in the overwhelming majority of different types of situations. Images of a hemorrhage demonstrate a startlingly hyperdensity that stands in stark contrast to its surroundings [39]. Imaging using X-rays has had a significant impact on both the cognitive and functional structure of the field of medical research. The kind of radiation known as X-rays are responsible for the emission of electromagnetic waves. If we compare it to employing microwaves and light, we may say that it is similar. CXR is used to generate a two-dimensional picture by traveling through the body. This gives you an idea of what is happening on the inside of your body.

Different components of the body are shown in a range of grayscale and monochrome tones. This is because different organs absorb radiation at differing intensities, as is discussed in more detail in [40]. In addition, the magnetic resonance imaging (MRI) scan provides information on a broad variety of bodily structures, which is information that can only be obtained with the assistance of an X-ray [41]. The compression ratio between the medical photographs is shown in Table 2.1.

Table 2.1. Comparison of medical images (CT, MRI, and CXR)

	X-Ray	MRI	CT
Resolution	Normal	Best	Moderate
Speed	Short	Long	Moderate
Cost	Low	High	High
Data acquisition	Low	High	High
Effects	Ionizing radiation	No	Ionizing radiation
Availability	Maximum	Less than CT	Without much difficulty

2.3. CONCEPTS AND TERMINOLOGIES

This section clarifies the problem and its solution by defining key terms and concepts. Brain tumor photos are critical for native researchers who need to know how to recognize, evaluate, and analyze these images.

2.4. WHAT IS THE TUMOR?

There are many different types of tumors, and they may be found in the brain or elsewhere in the nervous system. Because of this, this area of the brain is known as an abnormality or aberrant.

Many of the characteristics of tumors and malignancies differ. Whether solid or fluid-filled, a tumor is a mass of aberrant tissues. Cancer is also known as neoplasm. It is possible to classify tumors as primary or secondary, depending on the specific kind. Cells from that organ are incorporated into the tumor. For initial tumors to grow slowly, the nervous system is a typical source of sustenance. Brain tumors known as gliomas have glass cells as their primary structural constituents and are often seen in the central nervous system [42].

The surrounding healthy cells are harmed by the unchecked growth of aberrant tissues in the brain. Here we have cancerous growth. The three basic types of cancerous tumors are benign, malignant, and premalignant. The phrase "benign" refers to a characteristic that is not malignant. Using the phrase "malignant" is a way to describe anything cancerous. Symptoms of pre-malignant cancer may reveal a precancerous characteristic. Secondary tumors are formed by using cells from various parts of the human body. Spread may happen very quickly. In other words, cancer cells are responsible for the development of secondary tumors. Therefore, tumors are not cancer, but rather the first stages of malignant cells. Tumor categorization is based on a number of variables, some of which are given below:

- The position of the tumor.
- The discovery of a tumor in the brain.
- Identification in the storage locker.

Tumors may also be categorized depending on the kind of cells they include.

- It's a tumor comprised of neurons.
- This is a tumor that is mostly composed of glial cells.
- A bacterial and cell-based tumor has developed.
- The brain tumor known as a meningioma is one of several types.

These are the most common pathology-based categories in the United States.

- Innocuous.
- The cancerous

These scans may show tumors in different areas of the brain in Figure 2.1.

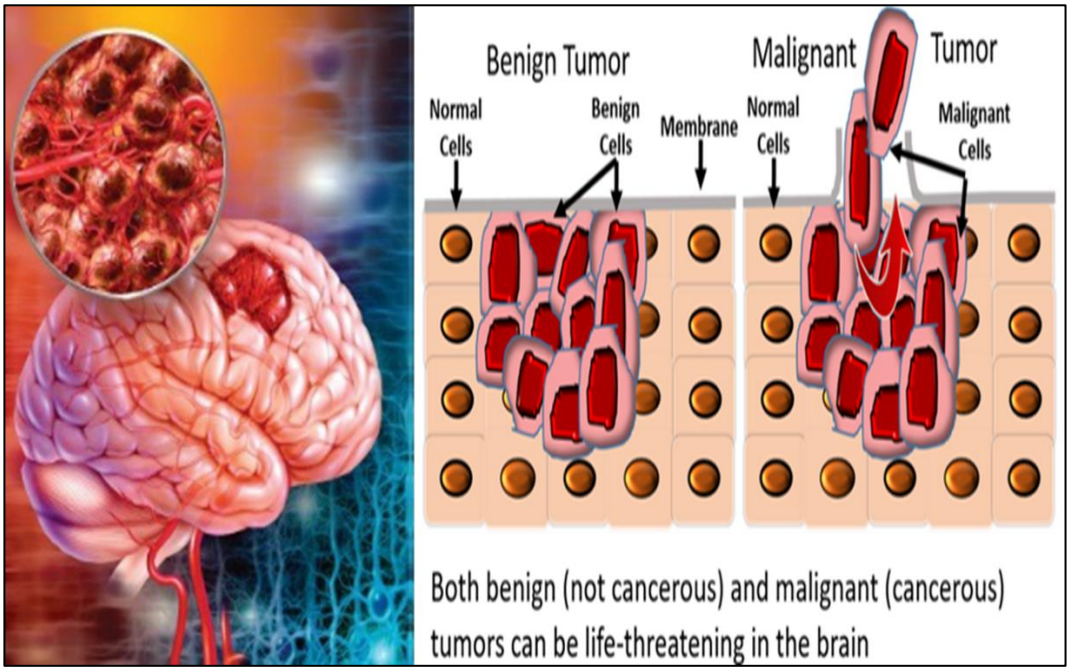

Figure 2.1. An example of a tumor-filled brain scan.

2.5. AN MRI IMAGE SHOWING THE TUMOR'S CHARACTERISTICS

Imaging using MRI rather than X-rays yields better results [43]. MR imaging, which may be used to diagnose sickness and make medical decisions, does not expose patients to harmful radiation. Brain cancers may be detected and diagnosed using pre-processed MR images [44]. Depending on the patient's requirements, a variety of MRI machines are used. Examples of MRI sequences that may be used as preprocessing inputs include T1, T2, and FLAIR. An understanding of the TE and the TR is necessary in order to appreciate the variety of MRI images. The interval of time between the transmission of an RF pulse and the reception of an echo signal is referred to as the TE (time of echo) [45]. The length of time that elapses between transmitting and receiving successive pulses is known as the repetition time, or TR.

T1-weighted pictures of cerebrospinal fluid [25]. Gray matter (GM) is darker than white matter (WM). Fat appears brighter in T1 images, which are better for examining the structure of the brain. A short TE and TR time (TR-500 msec, TE-14sec) is required to create the images (uses longitudinal relaxation).

In T2-weighted imaging [46], CSF and fluid have a higher signal intensity than tissue, making them seem bright. Images from T2 were made possible by the use of long-exposure timers (TR 4000 milliseconds, TE 19 milliseconds) (traverse relaxation).

T2 is a better option for edematous tissue since it is more apparent in liquid. FLAIR [47] does not utilize as much CSF fluid as T2, yet the anomalies are still clearly seen. An evaluation of cerebral edema may be done using this tool. An unusually lengthy TE and TR time is used to make images (TR-9000 msec, TE-114 msec) A comparison of the two sets of MRI images is shown in Figure 2.2.

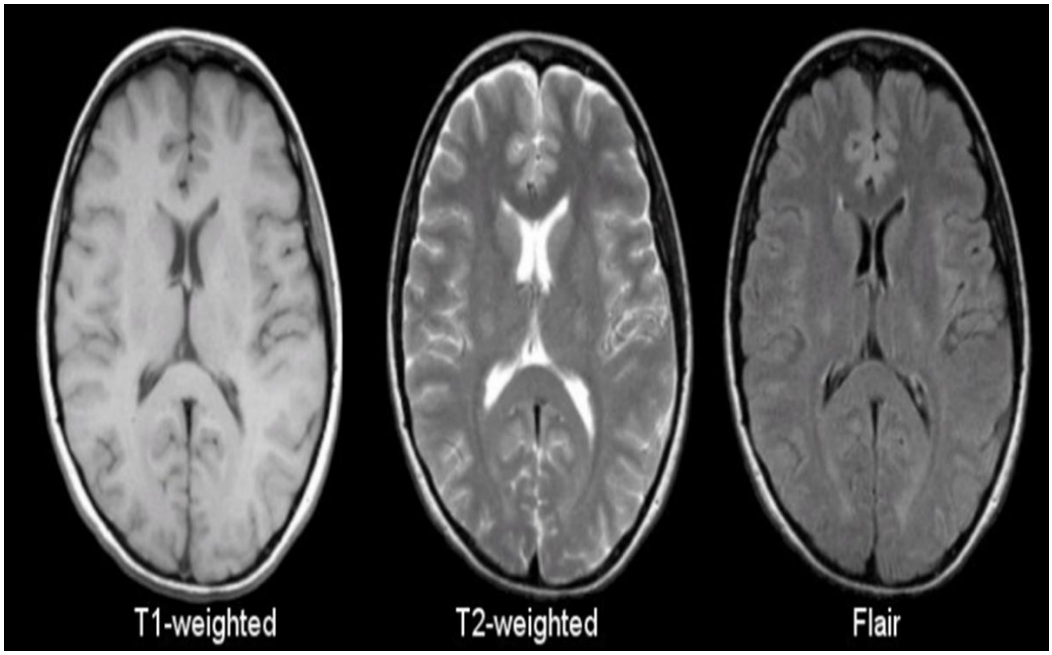

Figure 2.2. Type of MRI imaging technique

2.6. TECHNIQUES FOR IMAGE PROCESSING AND ANALYSIS

Because of the range of imaging modalities available, image processing is needed in order to make a proper diagnosis. This may be accomplished in a variety of ways, but

the focus of this study is on the most critical ones, such as filtering and image segmentation. These major methods may be used to correctly detect malignancies in brain MR images.

Enhancing medical pictures requires a preprocessing procedure. In this phase, we apply a number of restrictions that might have a negative impact on picture quality. A manual adjustment is part of our preprocessing. An important part of the preprocessing procedure is removing the film and skull sections from brain MR/CT images so that brain tumors may be more readily and securely recognized during post-processing [48]. Before moving on to the next step, which is needed to find brain tumors, the images are first segmented.

Utilizing the MRI images obtained with the flair and diffusion-weighted modalities, methods for inspecting the myocardial infarction lesion are suggested [48]. An example is shown in Figure 2.3 for image processing and analysis.

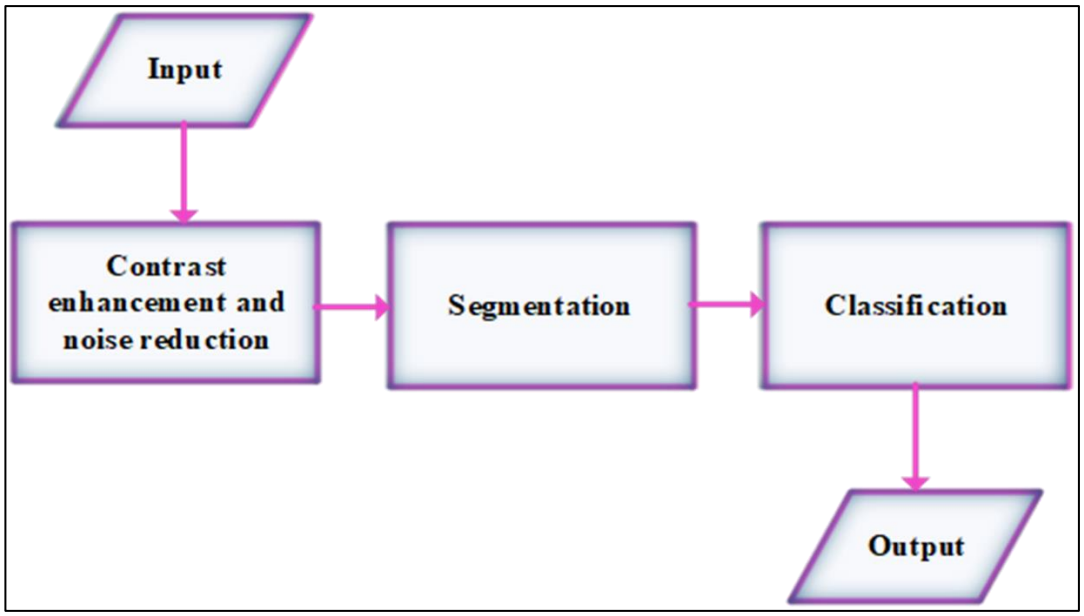

Figure 2.3. Analyzing and interpreting of medical images

2.6.1. Filtering and Noise Reduction

Filtering and de-noising the image is the first step in image processing. In order to remove any induced noise that may have snuck into the image during capture,

transmission, or compression, several restoration processes are utilized. By increasing the image's resolution, this method yields the best findings possible (See Figure 2.4)

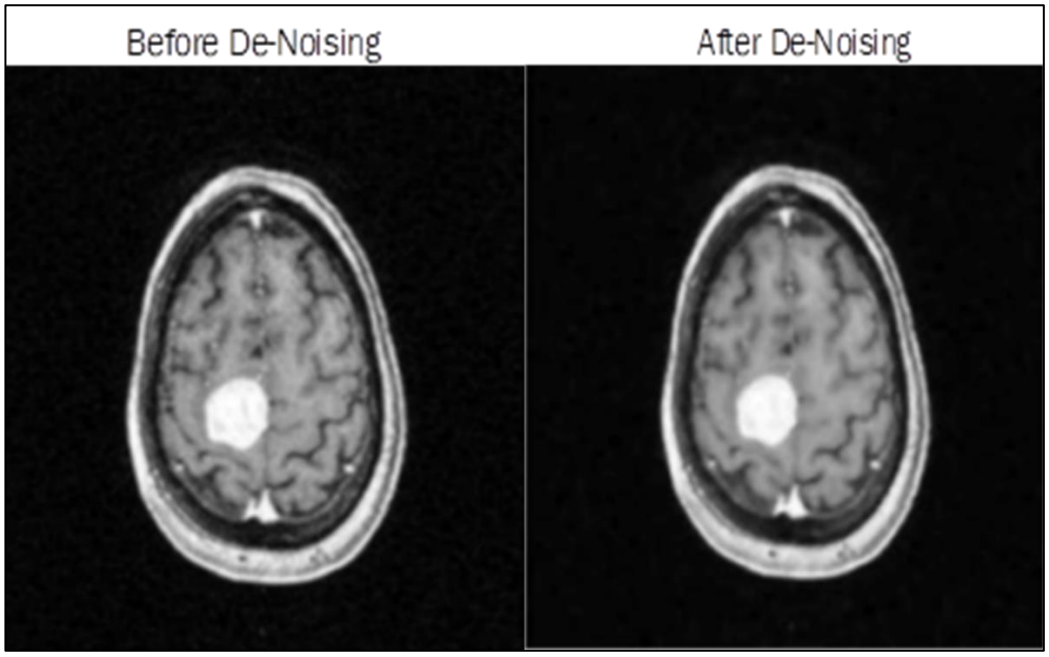

Figure 2.4. Image de-noising is seen in this example

2.6.2. The Process of Image Segmentation

Because of the range of imaging modalities available, image processing is needed in order to make a proper diagnosis. This may be accomplished in a variety of ways, but the focus of this study is on the most critical ones, such as filtering and image segmentation. These major methods may be used to correctly detect malignancies in brain MR images. Enhancing medical pictures requires a preprocessing procedure. In this phase, we apply a number of restrictions that might have a negative impact on picture quality. A manual adjustment is part of our preprocessing. An important part of the preprocessing procedure is removing the film and skull sections from brain MR/CT images so that brain tumors may be more readily and securely recognized during post-processing [49]. Before moving on to the next step, which is needed to find brain tumors, the images are first segmented.

Using MRI images from the flair and diffusion-weighted modalities, ways to look at the myocardial infarction lesion are suggested. In a number of medical imaging

techniques, image segmentation is critical. Multiple criterion segmentation algorithms will be applied after the improvement of medical images for brain tumors [50]. There are three basic categories of segmentation techniques for brain tumors in the clinic: manual, semi-automatic, and entirely automatic [51–54]. Color, texture, contrast, and gray level are all taken into account when dividing a photo into discrete portions. It takes a digital grayscale picture as an input to the operation. In order to do a CT scan or an MRI, Anomalies occur when anything goes amiss. Splitting a picture into smaller sections helps to reveal more information about the subject. In order to get the most accurate performance data, techniques like k-mean clustering and fuzzy c-mean are used [51].

A tumor of the brain is a mass of tissue that has grown in an uncontrolled manner within the skull, causing damage to the nerves and other vital organs. Unwanted cell progression may be caused by the proliferation or growth of neurons. It is summarized in Figure 2.5.

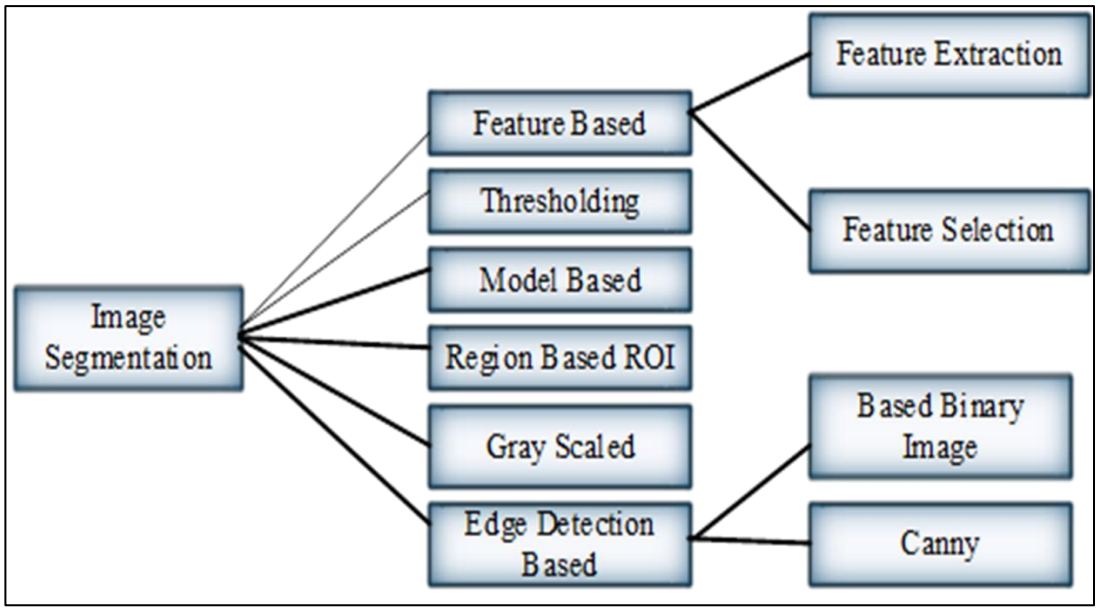

Figure 2.5. Types of image segmentation

The progression of a brain tumor necessitates a careful examination of the patient's symptoms. MRI is the imaging approach of select for locating tumors in the brain. It is incredibly difficult to reveal a tumor without damaging healthy tissue. An image processing approach was used to identify tumors, which included the capture,

preprocessing, and enhancement of the picture as well as image segmentation and classification [53].

2.6.3. Fuzzy C-Mean

The FCM method is one of the most effective data clustering methods. FCM, an unsupervised technique, may be used to do tasks such as factors that come, grouping, and segmentation, to name a few. It might be employed in horticulture construction, astronomy, biochemistry, image analysis, and medical evaluation, for example. In FCM, there are two or more data regions that can handle the partial volume impact (PVE). This is an iterative method that only examines the brightness of the segmented picture [54]. It is used to seek a succession of fuzzy clusters and their associated cluster centers in an incremental search to find the most accurate clustering of the data structure feasible. The latest batch of power points n is divided into a specified number of fuzzy sets using this method [55–57].

These techniques are used with an FCM algorithm to create segmented images. With FCM, you'll get a comprehensive look at all thirteen possible FCM segmentation methodologies all in one place. The emphasis of the review is on the use of FCM segmentation algorithms to brain tumors. A critical step in identifying brain cancers mechanically is fragmentation of the tumor. Because of the differences in brain structure, brain tumor segmentation is a difficult process compared to other forms of picture segmentation. The poor contrast of brain pictures makes this procedure much more difficult. Patients, clinicians, and medical providers all benefit from the early detection of brain tumors [57].

2.6.4. Threshold-Based Segmentation

Given the significance of picture segmentation, as well as its important role in the extraction of objects in the area of image processing, pattern recognition was developed. Essentially, it divides the input picture into many segments to facilitate finding the best match data to identify and extract the required region simpler. The most basic technique of segmentation is threshold-based segmentation. The

picture is separated into areas using one or more thresholds depending on density values [58–60]. A local threshold is used to segment photos with more than two sorts of regions corresponding to various objects. Light items in a dark backdrop are segregated based on the severity of the picture by setting a certain threshold value. Pixels over the threshold are considered as one in the picture, while those below the threshold are set to zero. The area of interest (ROI) is represented by pixels with a value of one, whereas the backdrop of the picture is represented by pixels with a value of zero. The current research study employs a threshold-based segmentation model, which allows us to increase the useful information by experimenting with the input picture at various thresholds and Max values. The threshold-based categorization separates the grayscale picture into two black and white blocks in the first phase. Different threshold values produced the greatest results in brain MRI scans. The Threshold-Based Segmentation approach is described in Figure 2.6 [60].

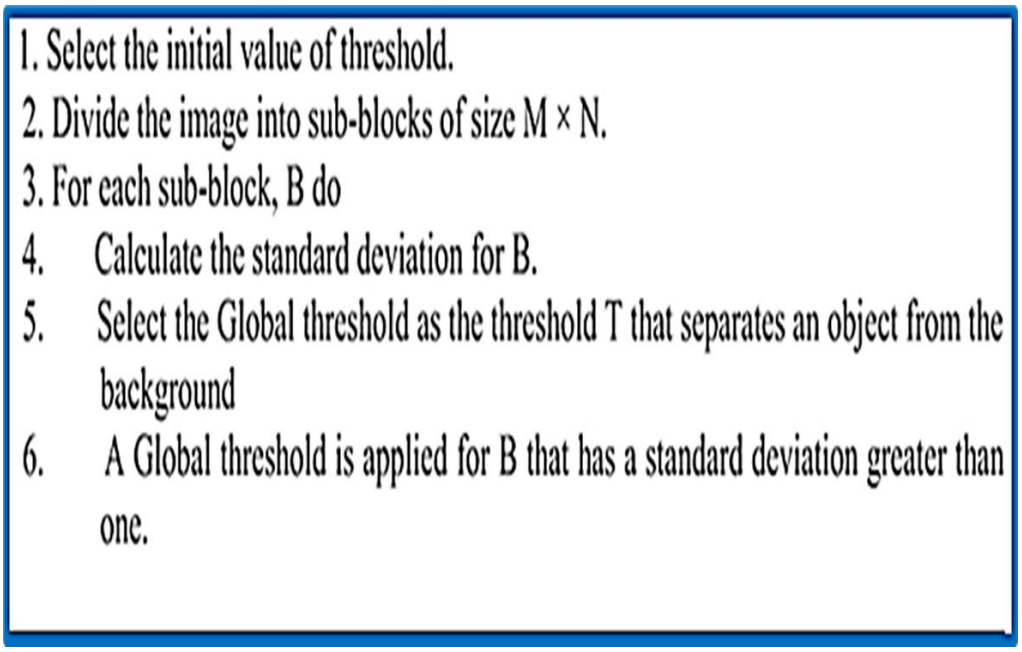

Figure 2.6. Threshold-based segmentation

2.7. IMAGES CLASSIFICATION

Using image classification, multiband raster images may be used to identify images. Each of these methods has its advantages and disadvantages. There are three ways to classify photos based on pixels: supervised (with user instructions), unsupervised (without standards), and hybrid [61]. In the software's calculations, Object-based image analysis, on the other hand, is a newer approach that relies on high-resolution photographs as input.

In recent years, a variety of techniques have been developed for detecting brain cancers in MRI images. Traditional image processing and machine learning based on neural networks are both included in this category. The tumor classification approach developed by Jun Cheng et al. [62] has two stages: the construction of an offline database and the retrieval of that information online. During the offline database phase, images of brain tumors are progressively evaluated. This includes tumor morphological operations extraction as well as distance metric learning. Brain scan input data is processed similarly and characteristics are obtained to compare to previously collected distance measurements in online learning environments. 94.68 percent classification accuracy may be achieved without using neural networks. The classification of brain tumors was accomplished by [63] using a Neural Network (DNN) with auto-encoders, on the other hand. Before the DNN layers processed the picture, image segmentation and feature extraction were carried out. Gray Level Co-occurrence Matrix (GLCM) and Discrete Wavelet Transform (DWT) were used to extract the image's texture and intensity-based properties. The classification was completed using DNN layers composed of two auto-encoders and a soft-max layer. The usage of Convolutional Neural Networks (CNN) with tiny 3 3 kernels to get to the er architecture and prevent overfitting is also being investigated by Pereira et al. [64]. Before launching into the CNN layers, they also looked at the usage of intensity normalization.

Unsupervised classification is a simple process since samples are not needed. A few basic processes are used to segment and classify the image. There are several instances of an unsupervised technique, including CNN, DNN, SVM, and more. For supervised

categorization, training sets are also necessary. For each training set, it creates a file with the description of each class that most closely matches the training set. Then, it uses that file to classify an image. The most often used supervised approaches are maximum likelihood and minimum distance classification. SVM is another well-known method for classifying images. For supervised classification, the best classification method is support vector machines (SVM). It is possible, however, to use SVM as an unsupervised method [65].

2.7.1. Review of Image Classification

An improved support vector machine (ISVM) classifier has been suggested to classify brain tumors in research [66]. SVM is used to identify abnormal cells in MRI scans as tumors in the proposed algorithm's dataset, which includes the processed image segmented using the K-mean technique. The experimental findings from the proposed approach were more accurate than those from other current systems. This method can detect tumors in less than a second, which decreases the execution time. Using k-means clustering, patch-based image processing, item counting, and tumor evaluation, the authors of [67] demonstrated a method for automatically detecting brain tumors in MRI scans. According to an analysis of twenty real MRI images, tumors of all sizes, even those with very low intensities or scales, may be detected in MRI scans. Robotic surgical technologies and treatment equipment automation are potentially possible integrations. In spite of tumor growth and variability in magnitude and location, a suggested MRI-based tumor classification technique proved effective.

It was proposed in [68] that a simple method for establishing a border around the tumor on MRI images may be used. According to this method, the k-mean strategy tackles some of the disadvantages of the usual KM algorithm, including the random initialization of centroid clusters and noise sensitivity. Our major objective is to combine the DPSO method and morphological reconstruction with the KM algorithm (MR). As part of the DPSO method, cluster centroids are generated from MRI scans of patients. It is also used to minimize noise and create clusters that are simpler to recognize.

The effectiveness of the suggested technique was evaluated in [69] by contrasting it with other methods of segmentation that are already in use, such as KM clustering and DPSO-based multilevel thresholding. Because of the effectiveness of the technique that is discussed in this article, it is now much simpler to identify tumors at an earlier stage. The purpose of this article was to propose a fresh method for segmenting MRI medical pictures. This technique differs from others that came before it in that it uses the novel K-mean clustering method, which incorporates photos that have the highest dominant gray level. This example shows how to choose k random pixels from a photograph, with the selection being determined by the predominant gray level in the image. compared well to the K-Means approach in terms of the accuracy of the images it produced, as shown by the results of the trials.

In the article [70], a hybrid technique that included the median filter and morphological processes was provided as a way to segment brain lesions in MRI and CT images. This was done in order to accomplish this task. The preprocessing of brain images using a median filter and k-means fragmentation helps reduce the amount of impulsive noise. When evaluating how well the proposed automated system performs on well-known datasets, one of the performance metrics that is utilized is how effectively the system can segment the data, and another is how long it takes to execute.

It has a 94 percent accuracy rate when contrasted with the manual delineation performed by an experienced radiologist [71]. The researchers want to look at the segmentation of tumors. Based on the fuzzy c-means methodology combined with skull stripping, which takes the kernel as its starting point. In order to improve the segmentation algorithm, geographic data is required so that many kernels may be blended together. We use global matching information across picture distributions rather than information on a pixel-by-pixel basis in order to save time during the computing process. In order to successfully eliminate tumor edema, co-segmentation via the graph cut approach is used to locate the precise location where edema and tumor meet. Because the tumor may be seen more clearly in [71], this procedure is the one that should be used. The simulations demonstrate that our strategy is better in terms of separating tumors and edema into the pieces that make up their wholes as an entire.

In medical image processing systems, fuzzy c-mean classification has been used for the purpose of identifying MRI brain cancers [72]. BCET is responsible for the labeling and enhancement of images, and one example of this is the use of a median filter. An agile edge detector is then utilized to construct an edge map of the brain tumor after the image has been segmented using the FCM clustering technique. The Canny methodology is superior to the BCET and FCM methods because it utilizes ideal input photos of higher quality and divides these images into homogenous portions. The end result is that those working in the medical field will be pleased with the findings, and the quality of the images is exceptional.

As a result of using the method described for minimizing noise and minimizing the impact of it, a stable edge map is created. [73] Proposed For the purpose of creating a hybrid better segmentation solution for medical pictures, fuzzy c-means and brain-storm optimization are both used. In the brain-optimization storm, cluster centers are given priority, just as they are in any other kind of swarm algorithm. The Brain-Storming Optimization (BSO) has shown some promising results, however the fuzzy approach takes a very lengthy time to determine the most optimal network layout. The suggested FBSO was efficient, durable, and primarily lowered the optimization algorithm segmentation time in the BRATs dataset. It also had 93% accuracy, 94% accuracy, 97% accuracy, 97% accuracy, and 95% sensitivity in the ideal solution.

According to reference [74], a Pre-smooth Non-Local Means filter (PSNLM) filter, also known as a fuzzy C-means algorithm, is used in order to determine the noise process by using an FCM algorithm reformulation FCM algorithm and PSNLM. The PIGFCM method makes advantage of this data because of the previous knowledge described above. It was shown that this method could reliably detect tumors by reducing the amount of time spent on picture de-noising, increasing the precision with which segmentation was performed, and doing all of this at a fast rate.

According to [75], FCM fragmentation may be utilized to distinguish between parts of the brain that contain tumors and those that do not have tumors. It is also possible to extract wavelet attributes using the multilayer discrete wavelet transform. The employment of a DNN is ultimately used for the goal of accurately identifying

cancerous growths in the brain. All of these other methodologies are analogous to KNN, Linear Discriminant Analysis (LDA), and Sequential Minimal Optimization (SMO). The categorization of brain tumors using DNN is exceedingly difficult and time-consuming, despite the fact that it has an accuracy rate of 96.97 percent.

Utilizing adaptive histogram equalization, as shown in [76], is one way to obtain improved contrast. After that, the tumor is separated from the rest of the image of the brain by employing FCM-based separation. Abnormal cells in the brain are sorted out once the retrieval of Gabor features has been completed. The KNN fuzzy classification is utilized as the last stage in the process of determining whether or not there are abnormalities present in brain MRI pictures. There is a considerable amount of complexity. However, the accuracy is somewhat lacking. In this research, the convolutional neural network was utilized to automatically identify a novel kind of brain tumor.

Table 2.2 contains an overview of current methods that have been developed to segment brain tumors on MRI and CT images.

Table 2.2. Summarizes studies that employed methods for brain tumor segmentation

References	Methods	Description	Images	Disadvantage
[20] **2018**	k-means clustering	The major purpose of this approach is to determine the boundaries of the tumor region existing in a defined MRI picture, to detect the tumor.	CT images	Losing some parts of the tumor, and that will increase the rate of segmentation error
[24] **2020**	Thresholding	Research on unsupervised techniques is the primary goal of this research.	CT images	Low segmentation accuracy on tumors located at the end of the brain
[25] **2018**	FPCM	Fuzzy-possibilistic C-means (FPCM) and shape-based topological characteristics are used in this study to determine the precise tumor location in MR images for brain tumor segmentation.	MRI images	It takes a long time and the accuracy of segmentation is low
[32] **2014**	k-means clustering	Fuzzy clustering algorithms are being used to reduce calculation time and improve segmentation accuracy.	MRI images	Low accuracy of the segmentation
[40] **2019**	Hybrid Clustering and Morphological Operations	Hybrid Clustering may be used for segmentation and extraction of brain tumors utilizing adaptive Wiener	MRI images	Low accuracy of the segmentation (losing more from the size of the

		filtering and morphological procedures, respectively.		tumor, and that will affect for identify the tumor class)
[54] **2020**	PCA with MFCM	This method's effectiveness in detecting distinct anomalies in actual MR images for the identification of intracranial neoplasms.	MRI images	The error rate of tumor segmentation is low and it is not compared with the recent methods
[56] **2021**	Cluster Validity Index-Based Fuzzy C-Means	The notion of cluster validity indices is introduced to estimate the appropriate cluster number in this study.	MRI images	The method was not tested on images having tumors located at the end of the brain that is more difficult to segment recently.

PART 3

METHODOLOGY

3.1. PROPOSED METHODOLOGY

Researchers apply typical computational approaches to the job of segmenting brain masses and constructing a prediction algorithm for MRI data in this portion of the study (e.g., whether an excised tumor is a glioma or a meningioma). In this article, we study approaches for segmenting MRI images that use an iterative and threshold-based approach. It is notoriously difficult to choose an appropriate global threshold between Fuzzy Clustering Means (FCM) and thresholding for the purpose of creating an optimal starting contour because of variations in gray levels in the area of pathology in images (for example, brain tumors). This is because of the strong relationship that exists between neighboring regions in subsequent medical images (MRI and CT).

In MRI pictures, the classification and identification of the margins of things of interest (such as the brain or the sick region of the brain) assists medical professionals in making a diagnosis (as gliomatumor or meningiomatumor). The use of segmentation allows for an exact determination of the size (outline) of these regions (tumors and normal areas of the brain). It has been shown that the data collected is both dependable and comprehensive thanks to the extensive number of accessible alternatives.

The quality of the pictures that are acquired via the use of medical equipment has a significant impact on the final outcomes. Because of the technical specifications of the devices, the pictures (or image groups) that are produced often include a significant amount of background noise. There are a few different approaches that may be used to recognize and classify brain tumors. The primary emphasis of the computational technique that we have proposed is on the precise segmentation of objects via the use of characteristics (in this case, brain tumors). We presented a method for processing

local objects (tumors) on MRI images in order to improve the diagnostic analysis accuracy on MRI images. This is because, as shown in Figure 3.1, noise in medical photos has the potential to skew the conclusions of the analysis. In light of this possibility, we presented this method.

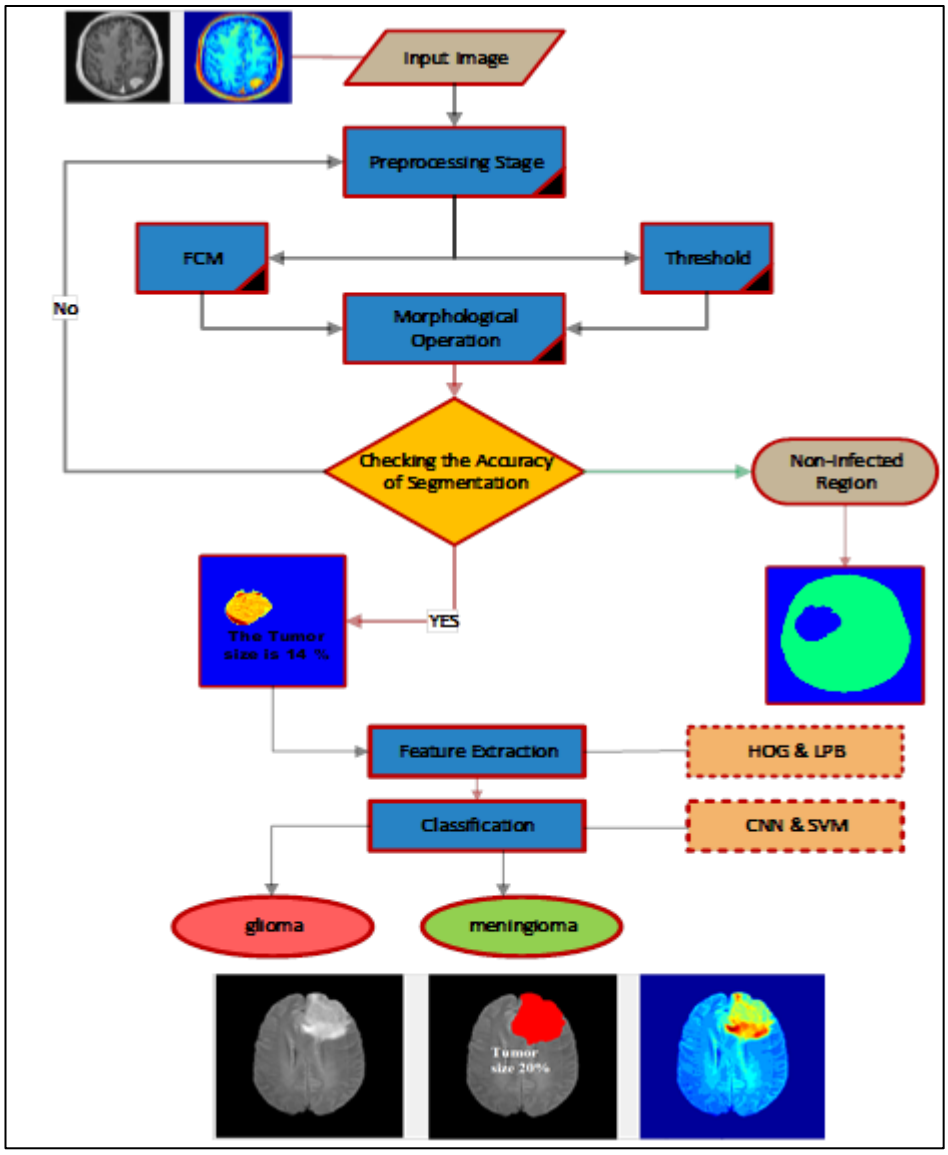

Figure 3.1. MRI brain tumor categorization block diagram

i. Preprocessing improves image resolution.
ii. Tumor segmentation measures tumor size by separating infected and uninfected areas.
iii. Morphological Operations remove undesired regions of binary images and smooth bulk boundaries.

iv. Feature Extraction improves tumor categorization accuracy.
v. Classification classifies segmented tumors as malignant or noncancerous.

In most cases, medical professionals will provide patients a report explaining the picture analysis as well as a link to the image in order to aid them in identifying the kind of tumor that they have. The cancer diagnosis process will be aided by the approach that we have developed, which will also make it possible for the system to be trained using a reduced amount of data. Following the completion of the validation process, the information will be included into a report about the state of health of the patient.

In many instances, the section of the picture that depicts the tumor stands out more clearly than the normal tissue that surrounds it. In this specific scenario, the created approach and code make use of the fundamentals of an algorithm that is designed to identify malignancies. During this time, the relevant portion of the paper may be attended to as needed. When processing data, analytical considerations are taken into account.

3.2. IMAGE CONTRAST ENHANCEMENT

In general, pre-processing is the step that improves the quality of MRI images of the local study area (such as brain tumors) so that they may be analyzed more thoroughly. In addition to this, a form is produced that may be further examined by either human eyes or automated vision systems. As shown in [77], preprocessing also has the effect of improving some MRI features.

After that, in order to improve the signal-to-noise ratio, we make use of an adaptive contrast enhancement technique that is based on the revised function (described in [78]). As a direct result of this, the first MRI scans will have a greater overall quality. Poor image quality is the most significant obstacle that must be overcome for accurate parameter extraction, analysis, and identification. Because of the inherent limitations of the imaging process, it is not very common for medical pictures to be contaminated by impulsive, multiplicative, or additive noise. This is because of the inherent

limitations of the imaging process. The authors of [37] suggested using a method known as the Contrast Balance Enhancement Technique (CBET) in order to boost contrast while simultaneously bringing attention to the region of concern. When it comes to medical imaging, contrast plays a significant role in highlighting the region of interest.

There is a technique that is referred to as contrast restricted adaptive histogram equalization that is discussed in the literature [79,80]. (CLAHE). This method was developed to assist medical professionals in making more accurate diagnoses by highlighting and rating important qualities that may be seen in medical pictures. The alternative technique for enhancing images known as unsharp masking has a lot of potential and holds a lot of promise. Even though this method makes use of a high-frequency emitter to enhance the appearance of edges and finer details, it is still quite susceptible to the noise that is present in the surrounding environment. The author of [81] demonstrated that a method known as the "invariant contour transform" (STICT) may be used in order to enhance the overall image quality of MRI images.

The procedure that we have outlined makes use of an algorithm (BCET). There is no effect that changes in the length or breadth of the histogram have on the contrast of the picture that is being entered ($I\ old$). In order to "fit" the image and get the answer, a parabolic function will be utilized. The following equation is a representation of the function known as a parabola:

$$I_{New} = a \cdot (I_{old} - b)^2 + c \tag{3.1}$$

The supplied data is used to calculate the coefficients a. The maximum output image value ($I\ New$) is used to calculate b and c, which are otherwise based on the smallest image pixel value ($I\ New$). The average output pixel is valued using the following formula:

$$b = \frac{h^2 \cdot (E - L) - s \cdot (H - L) + l^2 \cdot (H - E)}{2 \cdot \left[h \cdot (E - L) - e \cdot (H - L) + l \cdot (H - E)\right]} \tag{3.2}$$

$$a = \frac{H - L}{(h - l)(h + l - 2b)} \tag{3.3}$$

$$c = L - a(l - b)^2 \tag{3.4}$$

$$s = \frac{1}{N} \sum_{i=1}^{N} I_{Old}^2(i) \tag{3.5}$$

where H and L are the top and bottom values of the image being supplied. It is essential to take note of the fact that the letters H and L stand, respectively, for the brightest and darkest sections of the image. The symbol s denotes the size of a pixel on average, while the symbol e indicates the mean square sum of the source image.

3.3. BRAIN TUMOR SEGMENTATION METHOD

One common use of image segmentation is in the area of boundary and object detection (curves, lines, etc.). Segmentation of medical pictures to locate a specific feature is the first step [82,83]. (e.g, brain tumor using MRI images or other medical imaging techniques). This is because determining the best course of therapy should begin as soon as feasible.

Based on Otsu's extended fuzzy clusters and C-means, this thesis created a threshold recurrence approach for segmenting objects (tumors) and undamaged areas (brain) on MRI and CT images. Using this method, we can distinguish infectious from uninfected areas (see flowchart of the segmentation approach in Fig. 3.2).

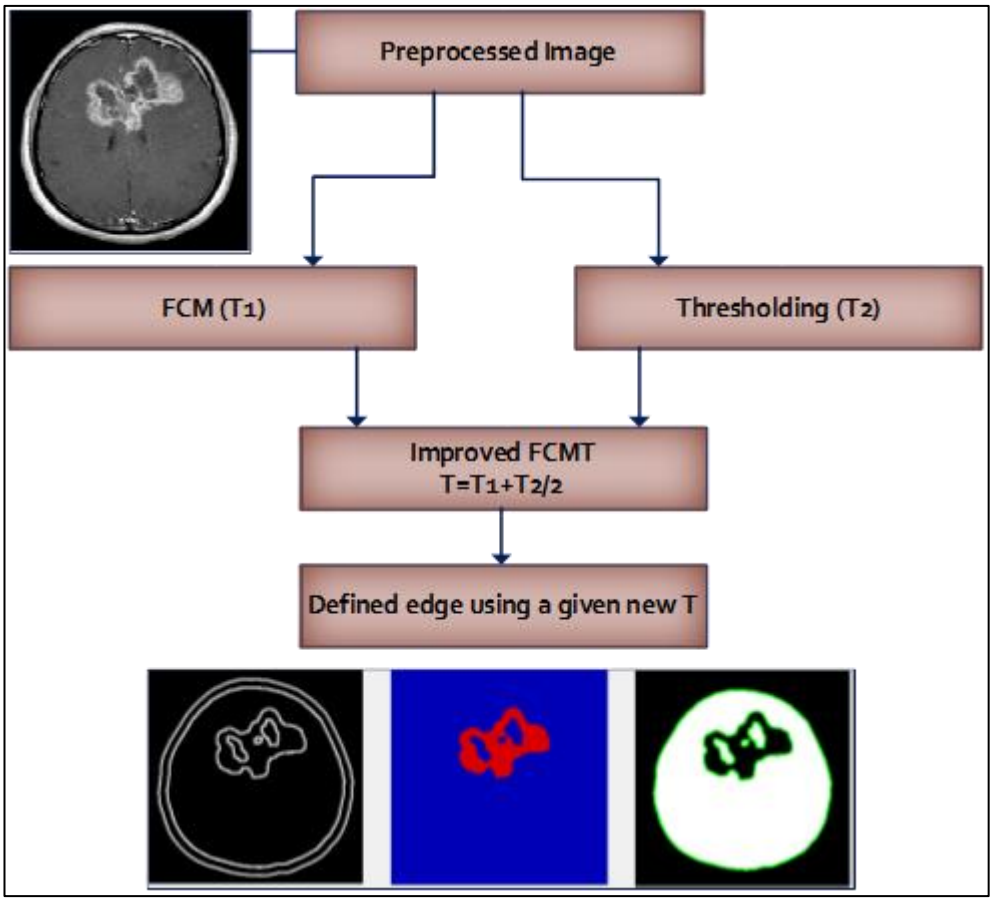

Figure 3.2. Developed brain tumor segmentation

In the field of medical imaging, image segmentation, also known as the process of extracting a Region of Interest (ROI) from a larger image, is very necessary. Several different methods of image segmentation have been used in order to separate certain organs and tissues for the purposes of diagnostic testing. This technique has a wide variety of applications, some of which include the detection of masses in mammograms, the registration of photographs, the analysis of cardiac imaging, the segmentation of cardiac structures, and many more [84,85]. Other uses include the automated classification of blood cells, study into the development of the brain and other animals, functional mapping, and edge detection on coronary angiography.

Let the intensity of the grayscale picture be expressed as a range of L values $[1, 2, \ldots, L]$. The fraction of dots that are a shade of p gray is denoted by xi (i). The sum of all possible points is denoted by the formula $X = x\,1 + x\,2 + +x\,L$. The distribution of the grayscale picture is interpreted as a frequency distribution of events:

$$p(i) = \frac{x_i}{X}, x_i \geq 0, \sum_{i=1}^{L} x_i = 1 \quad (3.6)$$

Each pixel in an image has two components—a foreground component (C 0) and a background component (C 1 with a minimum value of t). Pixels in levels $[1, 2, \ldots\ldots, t]$ are re-presented by C 0, whereas those at levels $[t + 1, \ldots L]$ are shown by C 1. The class occurrence probability and the median occurrence probability are defined by the following formulae.

$$w_0 = w(t) = \sum_{i=1}^{t} p(i) \quad (3.7)$$

$$w_1 = 1 - w(t) = \sum_{i=t+1}^{L} p(i) \quad (3.8)$$

$$\mu_0 = \sum_{i=1}^{t} \frac{i.p(i)}{w_0} = \frac{1}{w(t)} \quad (3.9)$$

$$\mu_1 = \sum_{i=t+1}^{L} \frac{i.p(i)}{w_1} = \frac{1}{1-w(t)} \sum_{i=t+1}^{L} i.p(i) \quad (3.10)$$

The overall average is defined:

$$\mu_T = \sum_{i=1}^{L} i.p(i) \quad (3.11)$$

and then we can find:

$$\mu_T = w_0\mu_0 + w_1\mu_1 \quad (3.12)$$

where w_0 and w_1 - denote the probabilities of the front and background areas. In addition, μ_0, and μ_1 represent the average gray level of the foreground and background gray image, respectively. Where the entire gray level image is defined as μ_T,.

3.4. FEATURE EXTRACTION

The preprocessed Computed tomography data in this investigation yields both local and global properties. HOG and LBP feature extraction methods are described in-depth in the following subsections.

3.4.1. HOG Features

The Histogram of Oriented Gradients (HOG) is used by object recognition systems to classify patterns in images. The frequency with which different gradient orientations occur in a given region of a medical picture is calculated. Easily and quickly, extract features with the help of the HOG feature extraction module. Given the simplicity of the underlying calculations, it is a far more expedient and effective feature descriptor than SIFT and LBP. It has also been shown that HOG features may be used as helpful detection descriptors. One of the most popular applications of this technology is in the realm of computer vision, namely in the realm of image processing. The image's form and look could be described using HOG. In this study, a 4-by-4 pixel cell size was employed to partition the picture and determine the edge directions. Histograms may be "normalized" to make them more reliable.

A local object's look and shape may be described with the help of the histogram of directional gradients since it uses the distribution of intensity changes or data to do so. By segmenting the image into discrete, interconnected sections called cells, a gradient direction histogram may be generated for each cell. Next, we utilize SVM to classify the fashion items in the F-MNIST dataset according to the retrieved photos' different properties. Before training a classifier and conducting an evaluation, it is required to do some preprocessing work on the collected picture samples to eliminate noise artifacts. Classifiers may be trained more effectively using improved feature vectors produced by pre-processing. Adequate preprocessing is necessary to decrease misclassification and increase identification rates. In the suggested research, fashion product identification is accomplished via the use of HOG-based feature extraction. HOG feature extraction is performed on 28 x 28 pixel wide images [86,87]. This data is combined to generate the description. By giving an estimate of the

intensity over a larger region of the image, known as a block, and then using this value to normalize each cell within the block, local histograms may significantly increase accuracy. The reversal of light and dark is enhanced by this normalization. Obtaining HOG characteristics may be shown as a series of processes in Figure 3.3.

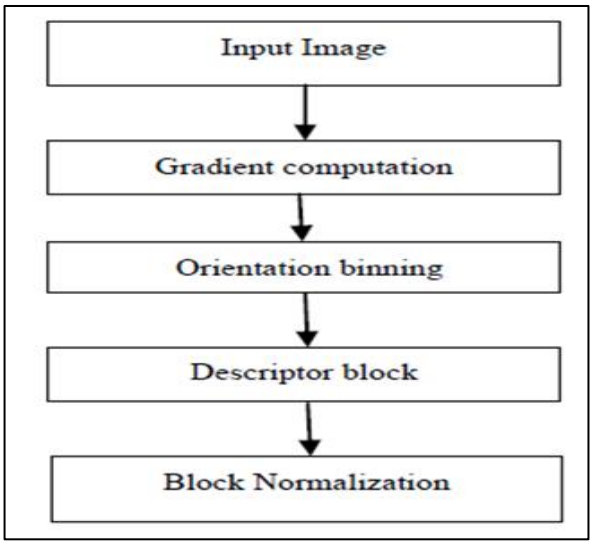

Figure 3.3. HOG feature extraction

a) Gradient Computation

Each cell contains a 1-D distribution of gradient or border orientation over its pixels, gathered by breaking the picture window into small spatial parts known as cells. Throughout the process of calculating, the grade values are kept track of. The most common method is to use the 1-D centered, pointed discontinuous derivatives mask in both the horizontal and vertical axes. To create the gradients, we employed background subtraction and then tested them with a variety of discrete masking derivatives. Color or intensity data must be filtered to guarantee the efficacy of the kernels in this approach:

$$A = [-1,0,1] \; and \; [-1,0,1]^T \tag{3.17}$$

b) Orientation Binning

The second stage of Feature Extraction involves calculating cells for use in statistical analysis. The values of the edge direction histogram channel are aggregated into orientation bins across cells, which are very small spatial areas, depending on the direction of the gradation element at their center. The shapes might range from square to round. Whether the gradients are unsigned or signed, the rotation bins are consistently positioned between zero and 180 degrees and between zero and 360 degrees, respectively. The images include nine direction bins, each 128 pixels on a side, for the [0°, 180°] range. The orientation bin for each pixel is determined by its alignment.

c) Descriptor Block

To modify the gradient strengths in the HOG features, cells must be joined together to form bigger, spatially linked blocks. The HOG specification is obtained by concatenating vectors of modified cell scatter plots for each area. Each cell is addressed several times in the final description, as seen by the frequent overlapping of these blocks. The basic geometric shapes that we see most often are the R-HOG and C-HOG rectangles and the circle. In this experiment, we use the rectangular R-HOG to determine the optimum parameters for 2x2 holding cells of 4x4 pixel cells with nine percentile channels. There are 36 HOG feature sets available from each CT scan image.

d) Block Normalization

There are four main methods for doing block equalization. A small constant (e) is placed in front of V, which represents all the histograms in a given block, and the non-normalized vector V is used to represent all the histograms in this block (the exact value, hopefully, is unimportant). After that, you may choose an adjustment factor from the following list:

$$L2-normal:\ f=\frac{v}{\sqrt{||v||2+e^2}} \tag{3.18}$$

L2-hys: L2-normal followed by clipping (limiting the maximum values of v to 0.2) and renormalizing, as in

$$L2-normal:\ f=\frac{v}{||v||1+e} \tag{3.19}$$

$$L2-hys:\ f=\sqrt{\frac{v}{||v||1+e}} \tag{3.20}$$

Taking the L2-normal, compressing the result, and then renormalizing may be used to compute the L2-his method. On the other hand, the wide variances in the depth of field lead to a wide range of gradient magnitudes. To solve this problem, the histograms of each cell are normalized by combining neighboring cells into a bigger block. Finally, the HOG-based bounding boxes are generated by joining all of the selected CT slices.

3.4.2. LBP Features

A Local Binary Pattern (LBP) is a description of the look of an image in the immediate vicinity of each individual pixel. The premise of basic normalization is that textures express a pattern and an intensity of a pattern, both of which are very small-scale features. For nearby binary patterns, the operator use an image block of size 3. To assign a label to the central pixel, we first threshold its value, then multiply it by powers of two, and then string these results together. Since the surrounding area is composed of 8 pixels, there are 28 = 256 different labels that may be generated by comparing the gray levels of the center and the surrounding area. The average and standard deviation of an image's LBP-Local properties are also used in during classification. LBPs work at the pixel level to convert a grayscale picture into a matrix of numbers. A description of the different components is provided by this label matrix. The system does this by identifying an appropriate mapping representation of the texture. The inclusion of visual descriptors like these is common in CVs since it helps

to quickly convey important information. When HOG feature descriptors are used, performance is dramatically improved.

A strong texture categorization characteristic, LBP is a feature descriptor. When interpreting CT images, it is critical to take texture into account. LBP has been found to be a powerful extension for classification problems because of its invariance to grayscale and rotation [88]. The radius N surrounding the central pixel is what determines the textural properties based on LBP sampling stations (neighborhood pixels) $LBP_{N,R}$:

$$LBP_{N,R}(x_c, y_c) = \sum_{k=0}^{N-1} s\big(x(k) - x(c)\big)2^k \ , \ s(x) = \begin{cases} 1, x \geq 0 \\ 0, x \prec 0 \end{cases} \quad (3.21)$$

where R is the circle's radius and N is the number of sample points at that radius. LBP pixel density is controlled by R, which governs the quantization of angular space. As a consequence, the accuracy of classification is strongly influenced by these two factors. X (K) and x(C) denote the values of the pixel K and the center pixel C, respectively. The function s guarantees that LBP's gray-scale and rotation invariants are invariant (x). In this case, s(x) has a value of 1 if it is larger or equal to the value of the pixel x (K). Otherwise, s(x) has a value of 0.

3.5. CLASSIFICATION METHODS

Prediction of tumor on medical images using extracted characteristics has been achieved using the SVM classifier (LPB and HOG). Non-probabilistically assigning new instances to one of two groups, the SVM is a kind of binary linear classifier trained using a collection of examples pre-divided into categories. For classification tasks in high or infinite dimensional space, support vector machines may be used to construct hyperplanes and hyperplane sets. SVMs are an effective supervised learning approach used in machine learning to discover patterns in data. If sufficient separation and the maximum distance to neighboring training data of any category are attained, the hyperbolic plane may be reached. Generalization mistakes may be mitigated by increasing the margin of error. Figure 3.4 depicts the maximum boundary classifier. Supervised learning makes heavy use of classifiers like support vector machines

(SVM), which may be used to both classification and regression [89,90]. The Supporting Vector Machine may be helpful in many different types of recognition tasks, such as facial recognition, textual task completion, and others. When put to action in realistic situations, it succeeds admirably [91]. In this part of the lesson, we will train and test using SVM. The method was applied to the fashion pictures in the F-MNIST database, classifying them in HOG feature space using a multiclass support vector machine classifier. Rows of 1296 by 1296 HOG features are used to fill the whole feature space. Figure 3.3 depicts the SVM classifier's schematic representation.

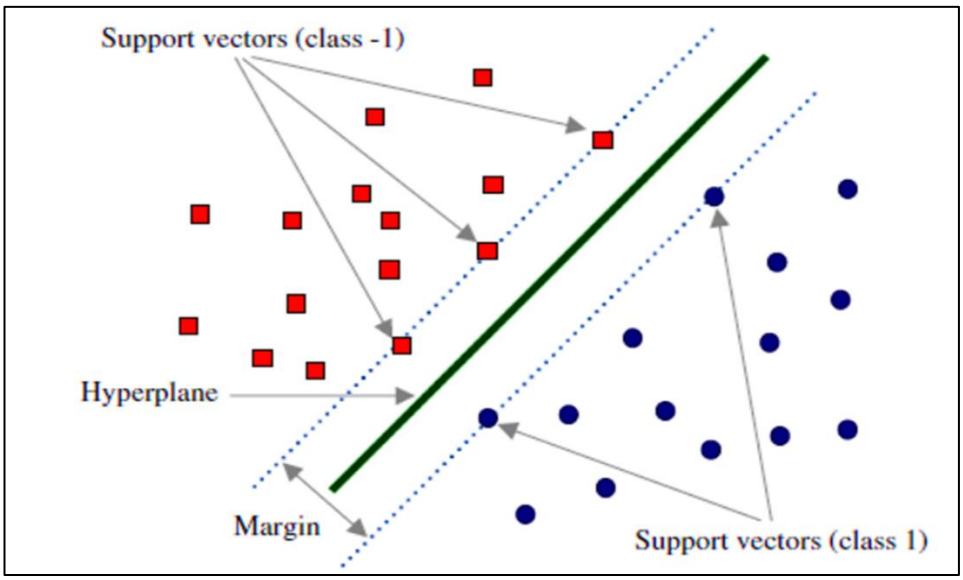

Figure 3.4. Maximal Margin Classifier

3.5.1. Support Vector Machines

Instead of creating many binary classifiers, it makes more sense to do a single optimization technique to separate all of the categories [91]. All k-binary SVMs may be learned at the same time using these techniques, which offer a clear goal variable and maximize offsets from each category to the remaining items for a k-class problem. Assuming a labeled training set, $\{(x_1, y_1), \ldots . (x_n, y_n)\}$ of cardinality l, where $x\_i \in R\hat{}d \; and \; y\_i \in \{1, \ldots, k\}$, the formulation proposed in [92] is given as follows:

$$\min \frac{1}{2} \sum_{m=1}^{k} W_m^T W_m + C \sum_{i=1}^{1} \sum t \neq y_i \tag{3.22}$$

$$W_m \in H, b \in R^k, \aleph \in R^{lxk}$$

subject to $W_{y_i}^T \varphi(x_i) + b_{y_i} \geq W_t^T \varphi(x_i) + b_t + 2 - \aleph_{i,t}$ (3.23)

$i = 1, \ldots., l, t \in \{1, \ldots., k\} \setminus y_i.$

The result of the decision is:

$$\arg \_max_m f_m(x) = arg_{max\ m\,(W_M^T \varphi(x) + b_m)} \quad (3.24)$$

3.5.2. Modified CNNs Model

We found that detecting photos with fine details is difficult via our investigation (as tumor is glioma or meningioma). Instead of being very like Res-Nets or Res-Next [65] models, the classification model should have a framework that can capture and learn tiny alterations. Figure 3.5 is an illustration of the proposed model used in this study. Specifically, the proposed model makes use of four convolutional layers. To standardize the inputs, the batch normalization method is used, which has additional benefits including reducing training time and increasing the model's stability. Leaky-Re-LU modifies the original Re-LU method to shield neurons on their way out of the cell. In all our pooling processes, we use the Max-pool method. In order to reduce the size of an input, Max-pool selects the largest value inside the region specified by its filter. The proposed model completes the glioma-tumor or meningioma-tumor and regular classification tasks while dealing with two classes. Whether brain tumor is labeled as glioma-tumor or meningioma-tumor, the same model is used to do the classification task. As a final step, Figures 3.6 provide the model's layer details and layer settings. There are 1,050,226 parameters in the learning model that was built. Weight updates, cross entropy loss function, and selective learning have all been implemented using the Adam optimizer.

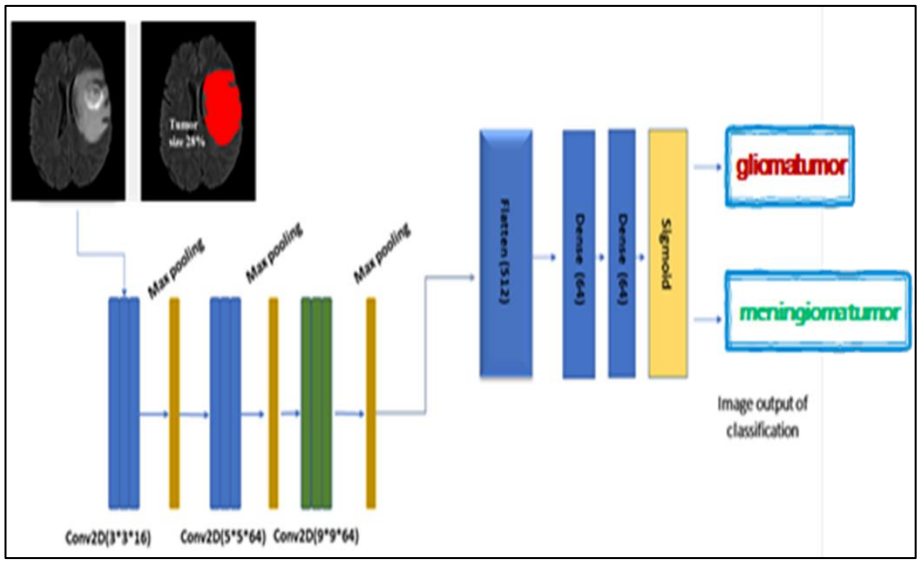

Figure 3.5. Modified CNNs Model

Layer (type)	Output Shape	Param #
conv2d_6 (Conv2D)	(None, 254, 254, 16)	448
max_pooling2d_6 (MaxPooling 2D)	(None, 127, 127, 16)	0
conv2d_7 (Conv2D)	(None, 123, 123, 16)	6416
max_pooling2d_7 (MaxPooling 2D)	(None, 61, 61, 16)	0
conv2d_8 (Conv2D)	(None, 53, 53, 16)	20752
max_pooling2d_8 (MaxPooling 2D)	(None, 26, 26, 16)	0
flatten_2 (Flatten)	(None, 10816)	0
dense_4 (Dense)	(None, 64)	692288
dense_5 (Dense)	(None, 2)	130

Total params: 720,034
Trainable params: 720,034
Non-trainable params: 0

Figure 3.6. Model Summary

The purpose of using these two examples is to assist radiologists in prioritizing glioma-tumor or meningioma-tumor patients for testing and treating infections based on their unique etiology. With these needs in mind, we created the CNN-MRI architecture, which comprises of three parallel layers with 16, 64, and 64 filters in each layer, all of which are different sizes (3-by3, 5-by-5 and 9-by-9). The coevolved pictures are then

subjected to batch normalization and rectified linear unit, followed by two types of pooling operations: average pooling and maximum pooling. The rationale for employing different filter sizes is to identify local features with 3-by-3 filters and somewhat global features with 9-by-9 filters, while the 5-by-5 filter size is to detect what the other two filters miss.

PART 4

RESULTS AND DISCUSSIONS

4.1. DATA BASE

Here, we take a look at the Chinese hospital's given clinical statistics on brain tumors. This chapter's goal is to evaluate the outcomes of presented approaches for segmenting and classifying glioma brain tumors by doing further validation using a realistic clinical dataset. In addition, this chapter investigates whether or whether the presented techniques may be used to segment a stroke lesion, another kind of brain tissue damage. In this preliminary study, we compared two datasets' analyses of the items (for example, brain tumor extraction and the prediction of whether it is a glioma tumor or a meningioma tumor). Our first dataset is the Digital Imaging Commons (DICOM) [85,93]. The researchers examined 150 images of brain tumors from the DICOM collection in order to get their conclusions.

A database of images was utilized by researchers from Nanfang Hospital and General Hospital, Tianjin Medical University, China. These images were slices taken from MRI scans performed between 2005 and 2010. This study also included supplementary research. The first online edition was released in 2015, and the most current version was finished in 2017 [94]. Only 708 of the slices showed pituitary adenomas, whereas the other 1,426 included meningiomas, gliomas, or both (930 images). Sagittal (1025 photographs), axial (994 pictures), and coronal scans were conducted of 233 people (1045 images). Figure 4.1 depicts potential subtypes of cancer along a variety of axes. Extreme scarlet coloring may be seen near the tumor's borders. There are limitless cameras watching everyone.

.

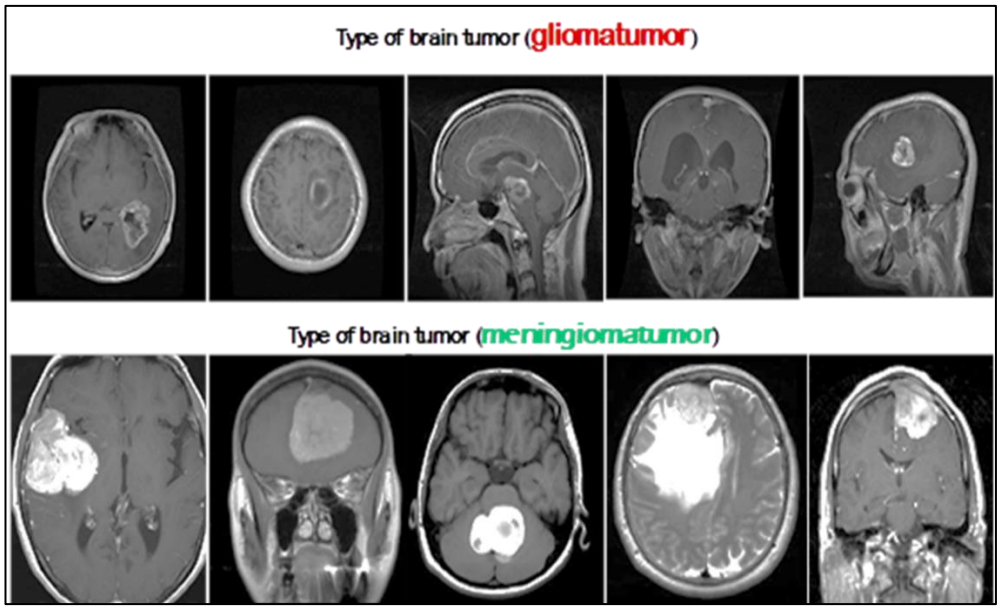

Figure 4.1. Normalized MRI scans depicting various tumor forms on various planes

4.2. SEGMENTATION RESULTS

We aimed to demonstrate that the modest architecture's performance was on par with that of larger, more involved designs. Reduced time and energy spent on image processing are two benefits of using an FCMT to differentiate between infected and healthy brain tissue and tumors. This is an important issue to fix since it hinders the system's use in clinical diagnostics and on software platforms where resources are scarce. The system must be adaptable if it is to be utilized in routine clinical diagnosis.

The results of applying various applications of BCET are presented in Figures 4.2. This is due to the fact that the MRI scan comprises varying contrast and, in this case, categorization rather than a perfect nomogram. Figures 4.2 also displays the outcomes of using other criteria.

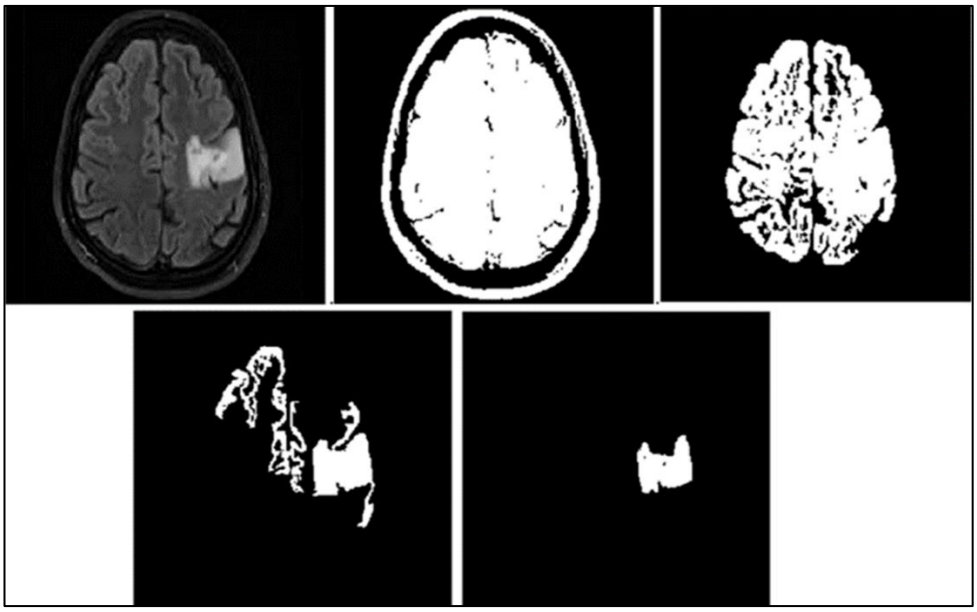

Figure 4.2. Results of using different mean value of BC for accuracy of tumor extraction: a) input image, b) BC mean value=120, c) BC mean value =100, d) BC mean value = 80, e) BC mean value = 50

In accordance with the proposed technique, a case study of the manufacturing and processing of a contour map is shown in Figure 4.3. All of the preceding are examples of what a brain tumor may look like, and they're all in the figure. Pictures (a), (b), and (c) were used for pretreatment; images (d) and (e) showed the results of localization using our approach (FCMT); images (f) and (g) showed the combined image and color map; and images (h) and (g) showed the end-edge map for the brain and tumor areas.

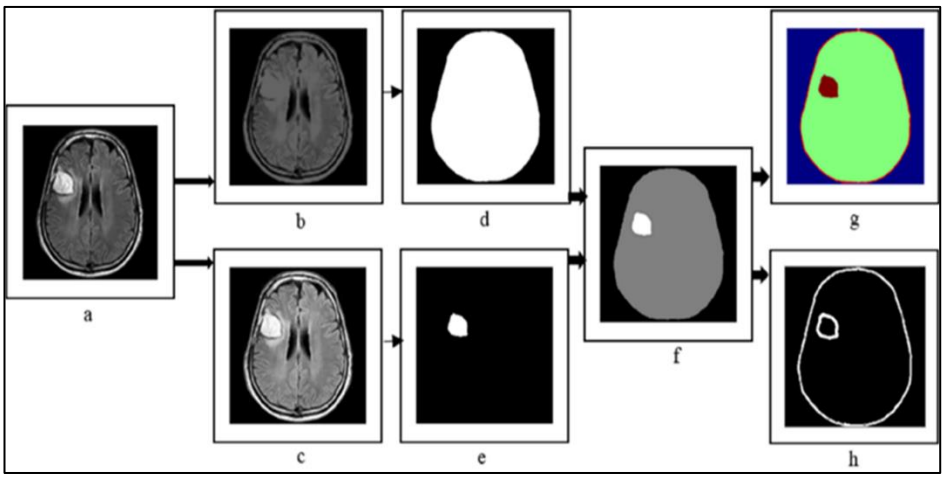

Figure 4.3. The combined segmentation methodology example for tumor and normal brain extraction

During the tests, a broad variety of 256-by-256-pixel images were used, each representing a different scenario. These results demonstrate the findings of some of the segmentation as well as the detection of brain tumors. The results of a computer experiment on the segmentation and detection of brain malignancies are shown in Figure 4.4, which shows many instances of brain MRIs that were acquired throughout the course of the experiment. It is also possible to note that the degree of brightness and contrast of the picture shifts from one image to the next, with the original shots showing in the top row, arranged from left to right. You may make this observation by looking at the images in the sequence shown above.

The first column contains the original photographs, and the second column contains the image results that were obtained after the preprocessing phase. These image results include a segmented tumor and are displayed in color with the assistance of a color map, as was discussed in the section that came before this one. The results of masking and processing can be found in the third column of this specific iteration of the calculation for the picture segmentation by areas. These results may be found in the very last column of the table (final contour images). It is also useful in calculating the area of the tumor, which is done in pixel units, and this is done by distinguishing between normal cells and malignant cells. Ultimately, this helps in measuring the size of the tumor.

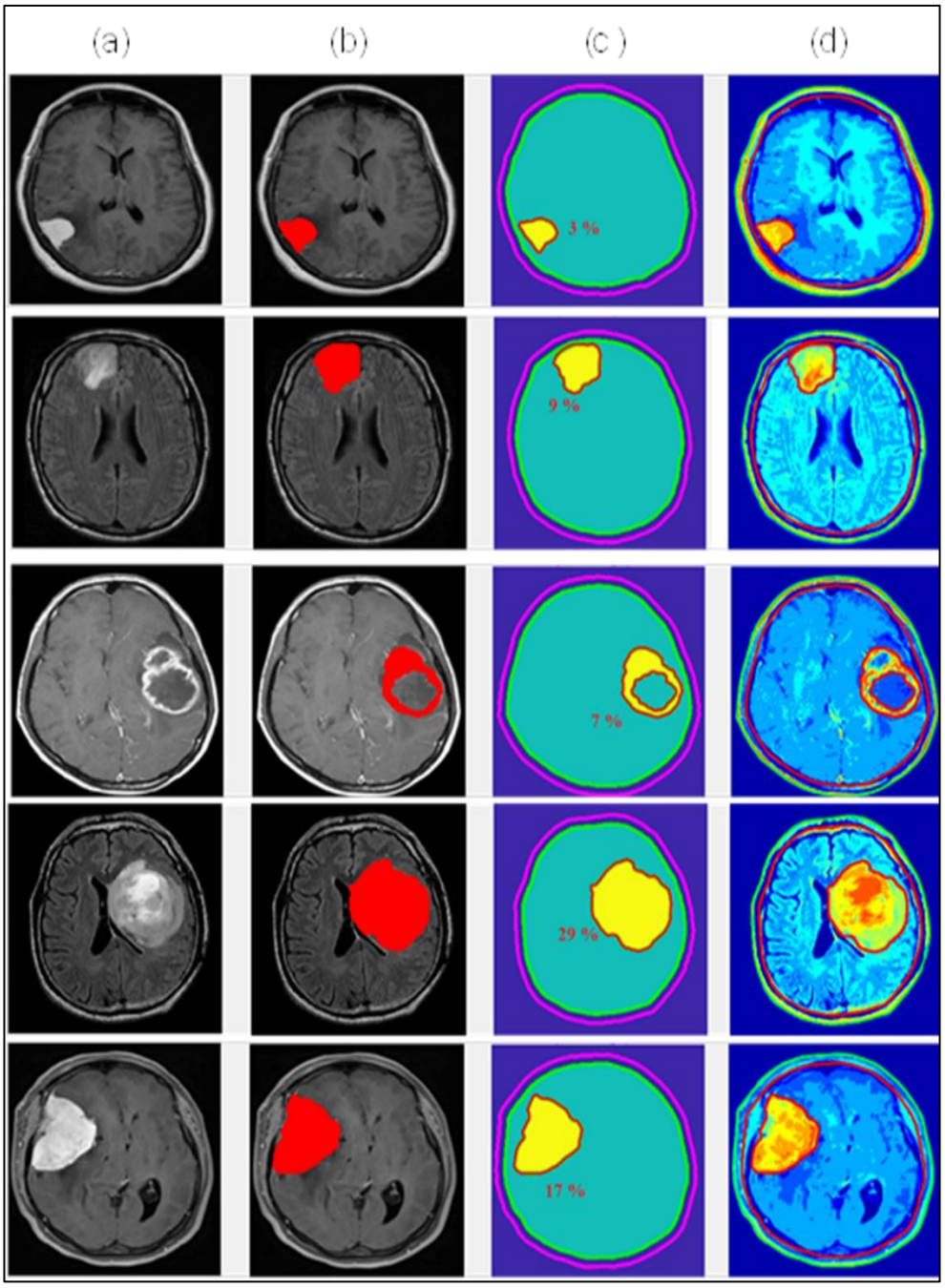

Figure 4.4. Segmentation results : In (a), the original picture is shown; in (b), (c), and (d), the experimental results show where the algorithm correctly located the item (a brain tumor and healthy brain tissue, respectively).

Figures 4.5 and 4.6 are the example of the developed software program under MATLAB 2021 platform that contain more than one results for tumor analysis, which helps the radiologist and specialist in diagnosing the disease and preparing a plan to treat the patient and keep him away from danger and maintain his health.

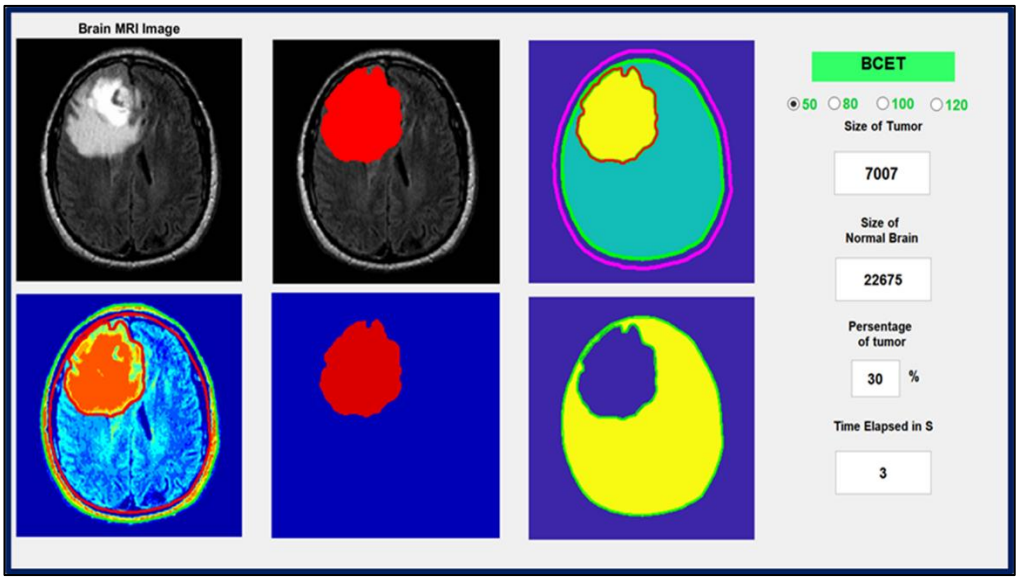

Figure 4.5. Example 1 of developed SW platform for mass analysis

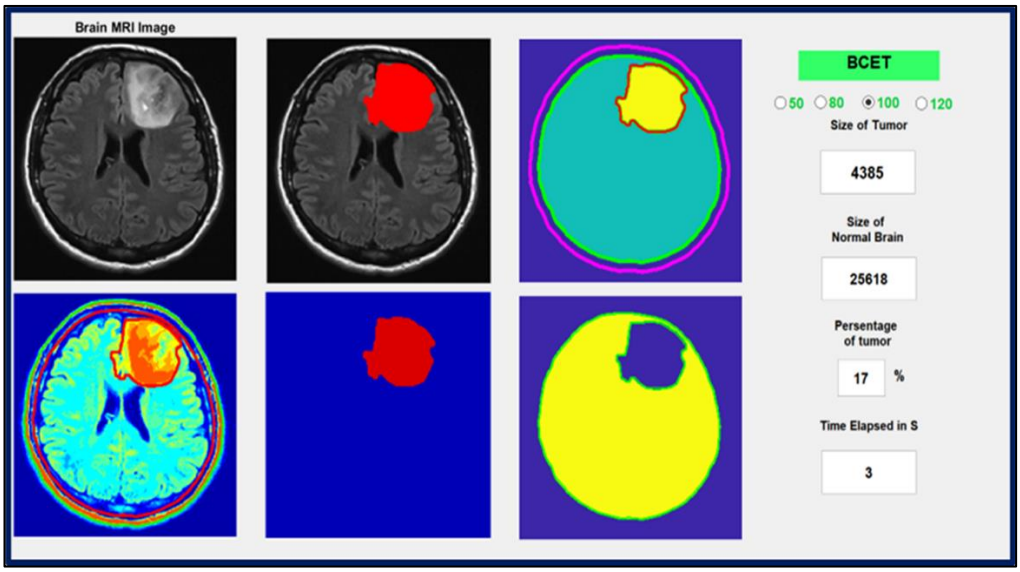

Figure 4.6. Example 2 of developed SW platform for mass analysis

As can be seen in Figures 4.4, our method successfully locates the tumor (and the healthy brain in the original input image). The state-of-the-art approaches, on the other hand, leave diagnostic uncertainty in portions of the Friday segmented picture that do not contain malignant tissue. Contrarily, our method successfully identifies a healthy brain in the original image (no tumor boundaries and normal areas of the brain). The visual analysis findings demonstrate the superiority of our technology over other approaches in terms of its ability to identify cancerous from healthy tissue. When tested against the following criteria, our method not only successfully delineated the

mammary gland's perimeter but also the normal brain tissue around it.

The accuracy of an image or signal is usually measured with Root mean square error (MSE). The purpose of measuring the accuracy of an image or signal is to determine the similarity between two images, and it can be measured by providing a quantitative estimate. In calculating the MSE, one of the images is assumed to be the original, whereas the other is distorted or processed in one way or another and is defined as:

$$MSE = \frac{1}{N}\sum_{i=1}^{N} E_i^2 = \frac{\|E\|^2}{N} \tag{4.1}$$

Maximum signal power divided by distortion noise power yields the peak signal-to-noise ratio, abbreviated PSNR. Use this formula to find out how much each variable affects the accuracy with which a signal is represented. This is commonly referred to as the "decibel level" when contrasting two images. Since the dynamic range of the signals is so great, the peak-to-average signal-to-noise ratio (PSNR) is commonly expressed as a logarithm of the decibel scale. The quality settings let a large range of values, from the very highest to the very lowest, to be considered, all within this dynamic range.

Lossy image compression codecs are measured against the standard of the Peak signal-to-noise ratio. Prior to and during compression, this ratio is evaluated. Assume the signal is the raw data and the noise is any mistakes introduced by data transformations such as compression and distortion. In contrast to compression codecs, which are optimized to minimize data, the peak signal-to-noise ratio (PSNR) is a measure of reconstruction quality that is roughly indicative of how humans would perceive it.

PSNR values may range from 30 dB to 50 dB for 8-bit data representation and from 60 dB to 80 dB for 16-bit data representation when discussing the quality deterioration that occurs during the compression process of still images and moving images. It is generally accepted that 20-25 dB of quality is lost during wireless transmission [80]. PSNR may be calculated using the following formula:

$$PSNR = 10\log_{10}\left(\frac{(2^n-1)^2}{MSE}\right) = 20\log_{10}(2^n-1) - 20\log_{10}\left(\frac{\|E\|}{\sqrt{N}}\right) \tag{4.2}$$

Perception-based Structural Similarity Index Method (0-1). Deterioration of a picture is seen here as a shift in how its structural details are read. Important perceptual facts like brightness masking, contrast masking, etc. are also involved. The phrase "structural information" refers to data that highlights the connections between, and among, neighboring or closely located pixels. These pixels, which are very dependent upon one another, correspond to additional crucial information about the visual objects in the picture domain. When an image's distortion is less noticeable towards the image's borders, this is known as luminance masking. Contrast masking, on the other hand, is a technique that makes distortions in an image's texture less obvious. The SSIM predicts how an image or video will be received. The two photos (the original and the restored one) are compared to determine how close they are. The following equation defines SSIM:

$$SSIM(x,y) = \frac{(2\mu_x\mu_y + C_1)(2\sigma_{xy} + C_2)}{(\mu_x^2 + \mu_y^2 + C_1)(\sigma_x^2 + \sigma_y^2 + C_2)} \tag{4.3}$$

It is also possible to evaluate the quality of a semantic segmentation by reporting the fraction of an image's pixels that were correctly labeled. In addition to class-specific reports on pixel accuracy, it is common practice to provide an overall summary for all classes.

To evaluate the precision of each pixel within a specific category is akin to assessing a binary mask. For a pixel to be considered "true positive" in a classification task, it must have been properly predicted to belong to the given class (according to the target mask), whereas a "true negative" must have been correctly detected as not belonging to the provided class. Because this metric is heavily weighted toward indicating how well you identify negative case, it might provide deceptive results when the category

represented is low inside the image. This may occur if the image's representation of the class is negligible (ie. where the class is not present).

$$\text{Accuracy} = \frac{TP+TN}{TP+TN+FP+FN} \tag{4.4}$$

Overlap accuracies were used to assess the precision of segmentation outcomes. For this evaluation, we used the well-known dice similarity coefficient (DSC; see also [47]). Here's how we've settled on a measure for success:

$$DSC = \frac{2TP}{2TP + FP + FN} \tag{4.5}$$

where TP, FP, and FN are the total number of positive, negative, and ambiguous voxels, respectively.

All of the PSNR, DSC, and SSIM variables benefit from this improvement, as shown by the evaluated performance factors. The proposed method pinpoints abnormal regions and malignancies in MRI scans with pinpoint accuracy. Table 4.1 provides a summary of the effectiveness of the collected images' periphery, broken down by tumor size and region free of disease (brain).

Table 4.1. Use the data in Figure 4.3 to calculate the efficacy of the excised tumors and pathology-free regions.

Images	**Tumor size %**	**PSNR**	**SSIM**	**DSC**	**Execution time in seconds**
Img 1	3 %	68.990	0.9765	0.9762	2
Img 2	9 %	65.004	0.9775	0.9839	3
Img 3	7 %	66.066	0.9800	0.9898	2
Img 4	29 %	67.03	0.9863	0.9850	3
Img 5	17 %	68.256	0.9896	0.9758	3

The shown technique yields a map of the borders of the target area (tumor region and normal areas) that is, on average, 4-7% more accurate. A smaller fraction of pixels are incorrectly identified as the affected region of the brain when using the recommended method. At noise levels under 10%, the difference is negligible. However, the sensitivity index reveals a more severe reduction while still falling below safe ranges.

Recent methods (since 2017) for medical image segmentation problems employing a convolutional neural network in combination with other segmentation techniques are summarized in Table 4.2.

When it comes to computer vision, one of the most challenging difficulties is getting a high degree of precision when segmenting an image. This is true even for experienced professionals. Numerous studies have shown that the use of learning strategies and models is helpful when working toward achieving this objective. learning-based conceptual and practical strategies that increase the quality and accuracy of with high accuracy segmentation have great potential for the future of computer vision.

Table 4.2. Clustering algorithms for medical images have advanced recently, using a variety of techniques

Year	Methods	Segmentation application	Modality	Accuracy (%)	Metric
2020 [14]	Genetic Algorithm	Brain tumor	MR images	92.03	DSC
2018 [38]	2 conductive U-Nets	Brain tumor	MRI-T1	94.30	DSC
2017 [60]	Thresholding + morphological image	Brain tumor	BRATS Brain Tumor	84.72	ACC
2018 [70]	K-Clustering – mean	Brain tumor	CT images	94.10	ACC
2020 [74]	CNN Approach	Brain tumor	MR images	91.05	DSC
2021 [55]	Modified fuzzy clustering	Brain tumor	MR images	90.50	DSC
2019 [68]	K-Clustering – mean	Primate Brain Extraction	MRI-T1	95.00	DCS
The developed method	FcMT	Brain tumor	MR and CT images	97.85	DSC
				97.74	IoU

Table 4.3 demonstrates that the created approach has a very high level of accuracy, with an error rate of just 3% to 4% when segmenting medical scans. We compared our method to five other models (Multi-Cascaded [94], Cascaded random forests [95], Cross-modality [96], Task Structure [97], One-Pass Multi-Task [98], and Cascade Learning model [99]) using both quantitative and qualitative metrics in order to gain a more in-depth understanding of the tumor segmentation performance.

Figures 4.7 and 4.8 provide the quantitative consequences of our different recommended structures, which serves as an additional illustration of these effects.

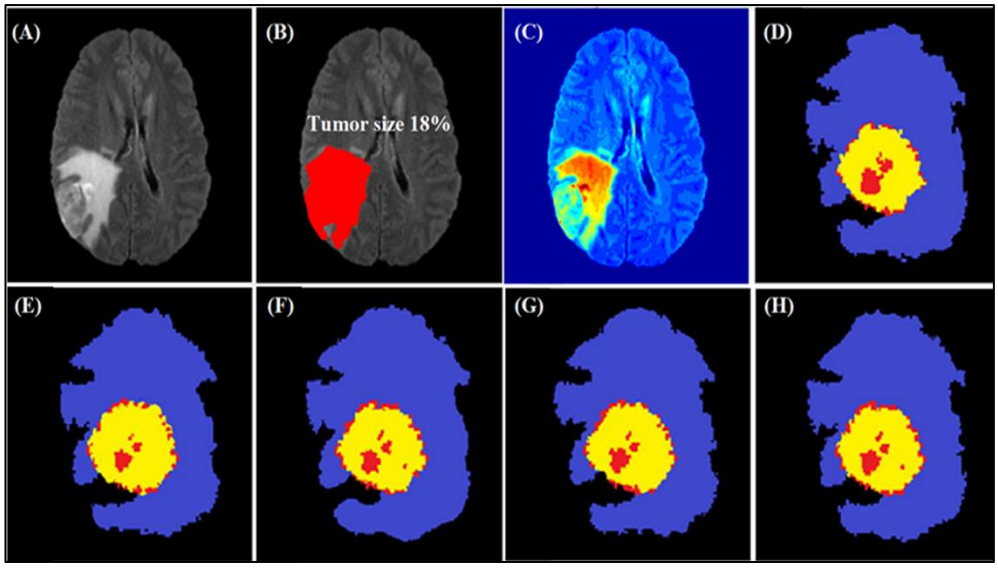

Figure 4.7. Localization of brain tumors using the accurate recommendations in conjunction with four other cutting-edge approaches on the BRATS 2018 dataset (the blue, yellow, and red colors are edema, enhanced, and core regions respectively). (A) The picture that was given to us, (B) and (C) our way, (D) Multi-Cascaded [94], (E) Cascaded random forests [95], (F) Cross-modality [96], (G) One-Pass Multi-Task [98], and (H) Cascade Learning model [99] are some of the models that have been developed.

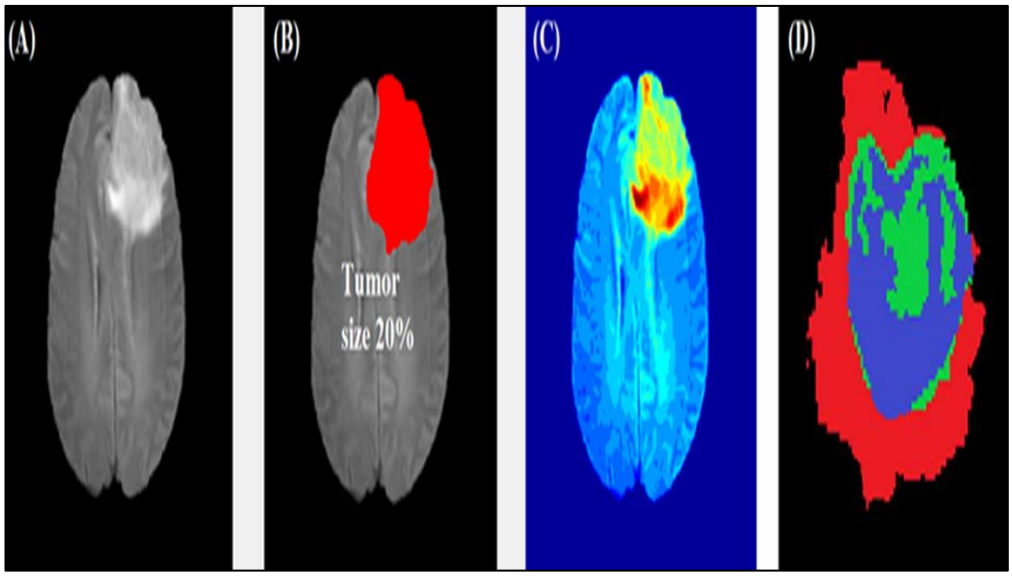

Figure 4.8. The results of segmentation of an infected area (a brain tumor) using our method and a Cascade Learning model on the BRATS 2018 dataset, with (A) the input image, (B) and (C) our method, and (D) the Cascade Learning model [99].

4.3. CLASSIFICATION RESULTS

The results of our method's application to the BRATS 2018 dataset are shown in Figures 4.7 and 4.8. As can be seen in the previous image, the boundaries of each region overlap with those of the others. Because of the disparity in value between the two, the demarcation line between the lesion core and the improving areas may be detected in the T1C images (the third column) with a high degree of accuracy owing to the fact that this line can be seen in the third column. This is due to the fact that it is possible to differentiate between the two. When talking about edematous areas, exacerbated edematous regions, or the margin of a tumor core, this is not the case. We find that a shallower CNN model is appropriate, provided that we adequately constrain our search space, taking into account the features that were discussed before for each modality.

Our algorithm still has some flaws that need to be worked out before it can handle tumors that are bigger than a third of the brain, despite the fact that the current technique beats the vast majority of the previously described models. This is due to

the fact that as the tumor grows, the predicted area becomes smaller, which results in worse than ideal outcomes when feature extraction is performed.

The SVM classifiers were trained using a dataset made up of MRI scans taken from the Digital Imaging and Communications in Medicine (DICOM) dataset in order to evaluate how well they could recognize images that included tumors throughout the training process. Table 4.3 presents, together with annotations providing more clarification, the findings and information that are pertinent to the categorization of brain tumors.

Table 4.3. SVM classifier of accuracy of brain tumor on CT images.

Images	**Quantity images**		**With combined feature (LPB+HOG)**		**Classification accuracy**
	Train	Test	Correct	Not correct	Accuracy
Glioma tumor	905	63	59	4	0.9365
Meningioma tumor	902	73	73	0	1.000
Total amount	**1807**	**136**	**132**	**4**	**0.9705**

Tumor predication is more accurate than not having a tumor, with an accuracy of 93% on photographs including a glioma tumor and 100% on images containing no meningioma tumor. Without a tumor, the accuracy is 100%. Table 4.4 demonstrates that when experimental studies employ integrated feature extraction, the average classification accuracy jumps to 97%. This results in tumor predication being more accurate than it would be without tumor.

When applied to MRI data, combined feature extraction has around a 6% error rate when attempting to predict the existence of glioma tumors. The Confusion Matrix, which combines both HOG characteristics and combination features (HOG + LPB), is shown in Figure 4.9 and is used for determining the prognosis of tumors.

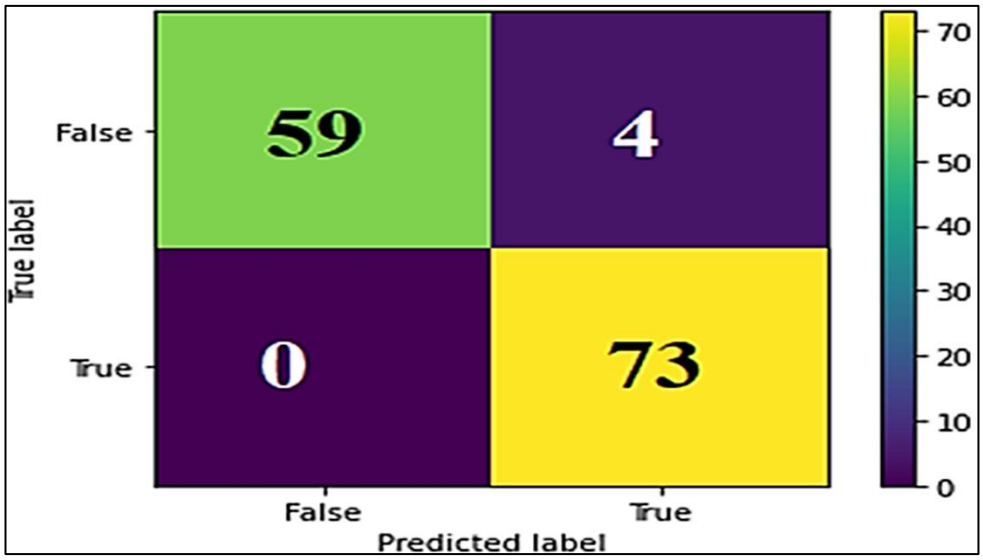

Figure 4.9. Confusion matrix of tumor predication using combined HOG+LPB features

It is clear from looking at Figures 4.6 that the updated technique for tumor predication, which combines HOG and LPB characteristics, provides a higher level of accuracy than just relying on HOG features alone. When compared to the standard technique, which has an error rate of 11%, the combination of LPB and HOG has a 3% mistake rate.

Table 4.4 displays the results of an assessment model that uses a matrix of precision, recall, and f1-score to measure the efficacy of a modified CNN in classifying tumors from the BRATS 2018 dataset (Glioma tumor or Meningioma tumor).

Table 4.4. Performance evaluation of modified CNN for tumor classification

Tumor Type	precision	recall	f1-score	Testing images
Glioma tumor	0.98	0.97	0.98	63
Meningioma tumor	0.97	0.99	0.98	73
accuracy		0.98		136

It can be shown in Table 4.5 that the accuracy of tumor prognosis is not bad. This is especially true for meningioma tumors, which are a subtype of glioblastoma multiform. This is the result of the experimental studies' average classification accuracy using the improved CNN, which was 98%.

The errors in the predication of glioma tumor in MRI images are about 4% and predication on meningioma tumor is 1%. Figure 4.10 shown the Confusion Matrix of tumor using modified CNN classifier (Glioma tumor or Meningioma tumor) on BRATS 2018 dataset.

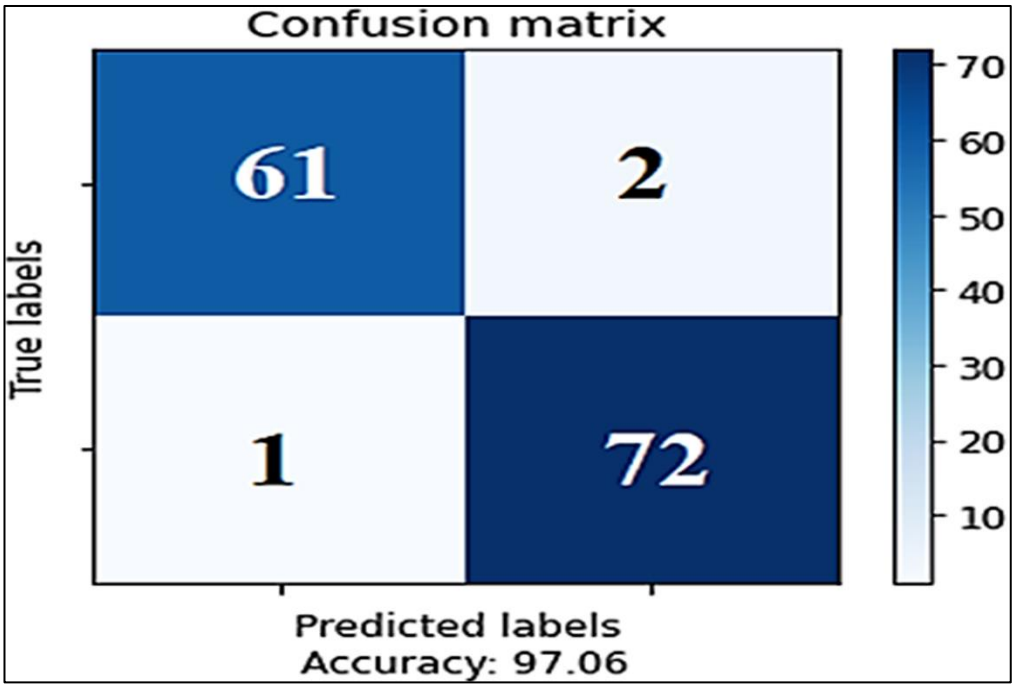

Figure 4.10. Confusion matrix of tumor predication using modified CNN

PART 5

CONCLUSION AND FUTURE WORK

5.1. CONCLUSION

Clinicians often do brain tumor analysis manually. Performing brain imaging analysis manually is time-consuming and a source of frustration as the science progresses. As a counterargument, computerized segmentation and classification facilitates neurologists' work since it facilitates their ability to reach a verdict. The field of brain tumor MRI image segmentation and prediction has experienced a lot of recent development thanks to the use of learning algorithms. Despite this, MRI remains a challenging subject with room for more research. The segmentation and classification processes greatly aid the medical professionals by allowing them to swiftly assess data and provide a second opinion based on automated discoveries. The primary focus of this thesis is on using machine learning to segment and classify malignancies (such as gliomas and meningioma's). Tumor segmentation makes advantage of image processing techniques established by FCMT, most notably contrast enhancement. LBP and HOG are utilized for feature extraction. Ensembles are the combination of these traits. Convolutional training is employed on this set of Ensemble Features for the neural network. A combined SVM using HOG and LPB features is proven to have an accuracy of 97%, while a retrained CNN model achieves a rate of 98%. Inaccuracies are uncovered at a rate of less than 2%. It's possible to improve the quality of this work by using ensembles classification techniques like using a convolutional neural network (CNN) with a number of different layer configurations or a convolutional neural network (DCNN) to get better results.

Images' quality and resolution, and hence a network's precision, are often impacted by the max-pooling process utilized in network topologies. Low-resolution feature maps have been the focus of almost all research until recently. There needs to be more

research done on this topic. Techniques that maintain an image's clarity and spatial recognition may be developed with more study. Most of the existing CNN-based treatments were created for a narrow subtype of the disease. Doctors would benefit greatly from a flexible DL-based framework that can identify various cancers. Most datasets used in academic studies have issues with data imbalance. One of the benchmark datasets, Brain Tumor Segmentation (BraTS), has 98% of its samples belonging to a single class and 2% belonging to another. Overfitting is inevitable when developing a model with such an unbalanced dataset.

5.2. FUTURE WORK

In addition, little research looked at how GANs and other advanced data enrichment techniques may be used to enhance brain tumor detection. In addition, little research have compared the efficacy of various data augmentation methods in identifying brain cancer. In addition, the majority of research didn't look at how various pre-trained networks at the state of the art may help in diagnosing brain cancer. Developing methods that combine cutting-edge data augmentation techniques with state-of-the-art pre-trained network architectures may help solve the issue of data imbalance and small-scale datasets in brain tumor diagnostics.

REFERENCES

1. "Brain Tumor Research. What Is the Difference between Primary and Secondary Brain Tumors?", **https://www.braintumourresearch.org/info-support/what-is-a-brain-tumour?** .

2. Luo, Q., Wang, Y., Fan, D., Wang, S., Wang, P., and An, J., "Prion Protein Expression is Correlated with Glioma Grades", ***Virologica Sinica***, 35: 490–493 (2020).

3. Paolillo, M., Boselli, C., and Schinelli, S., "Glioblastoma under siege: an overview of current therapeutic strategies", ***Brain Sciences***, 8 (1): 15 (2018).

4. Amin, J., Sharif, M., Raza, M., and Yasmin, M., "Detection of brain tumor based on features fusion and machine learning", ***Journal Of Ambient Intelligence And Humanized Computing***, 1–17 (2018).

5. Pedapati, P. and Tannedi, R. V., "Brain tumour detection using hog by svm", ***2018. , p. 48***, (2018).

6. Rao, C. S. and Karunakara, K., "A comprehensive review on brain tumor segmentation and classification of MRI images", ***Multimedia Tools And Applications***, 80 (12): 17611–17643 (2021).

7. Biratu, E. S., Schwenker, F., Ayano, Y. M., and Debelee, T. G., "A survey of brain tumor segmentation and classification algorithms", ***Journal Of Imaging***, 7 (9): 179 (2021).

8. El-Dahshan, E.-S. A., Hosny, T., and Salem, A.-B. M., "Hybrid intelligent techniques for MRI brain images classification", ***Digital Signal Processing***, 20 (2): 433–441 (2010).

9. Das, S., Chowdhury, M., and Kundu, M. K., "Brain MR image classification using multiscale geometric analysis of ripplet", ***Progress In Electromagnetics Research***, 137: 1–17 (2013).

10. Wang, T., Cheng, I., and Basu, A., "Fluid vector flow and applications in brain tumor segmentation", ***IEEE Transactions On Biomedical Engineering***, 56 (3): 781–789 (2009).

11. Al-Okaili, R. N., Krejza, J., Woo, J. H., Wolf, R. L., O'Rourke, D. M., Judy, K. D., Poptani, H., and Melhem, E. R., "Intraaxial brain masses: MR imaging–based diagnostic strategy—initial experience", ***Radiology***, 243 (2): 539–550 (2007).

12. Jiang, J., Wu, Y., Huang, M., Yang, W., Chen, W., and Feng, Q., "3D brain

tumor segmentation in multimodal MR images based on learning population-and patient-specific feature sets", ***Computerized Medical Imaging And Graphics***, 37 (7–8): 512–521 (2013).

13. Ortiz, A., Gorriz, J. M., Ramírez, J., Salas-Gonzalez, D., and Initiative, A. D. N., "Improving MRI segmentation with probabilistic GHSOM and multiobjective optimization", ***Neurocomputing***, 114: 118–131 (2013).

14. Amin, J., Sharif, M., Yasmin, M., and Fernandes, S. L., "A distinctive approach in brain tumor detection and classification using MRI", ***Pattern Recognition Letters***, 139: 118–127 (2020).

15. Chen, M., Yan, Q., and Qin, M., "A segmentation of brain MRI images utilizing intensity and contextual information by Markov random field", ***Computer Assisted Surgery***, 22 (sup1): 200–211 (2017).

16. Raja, P. M. S., "Brain tumor classification using a hybrid deep autoencoder with Bayesian fuzzy clustering-based segmentation approach", ***Biocybernetics And Biomedical Engineering***, 40 (1): 440–453 (2020).

17. Arunkumar, N., Mohammed, M. A., Abd Ghani, M. K., Ibrahim, D. A., Abdulhay, E., Ramirez-Gonzalez, G., and de Albuquerque, V. H. C., "K-means clustering and neural network for object detecting and identifying abnormality of brain tumor", ***Soft Computing***, 23: 9083–9096 (2019).

18. Huang, Z., Xu, H., Su, S., Wang, T., Luo, Y., Zhao, X., Liu, Y., Song, G., and Zhao, Y., "A computer-aided diagnosis system for brain magnetic resonance imaging images using a novel differential feature neural network", ***Computers In Biology And Medicine***, 121: 103818 (2020).

19. Kapoor, L. and Thakur, S., "A survey on brain tumor detection using image processing techniques", (2017).

20. Zeinalkhani, L., Jamaat, A. A., and Rostami, K., "Diagnosis of brain tumor using combination of K-means clustering and genetic algorithm", ***Frontiers In Health Informatics***, 7: 6 (2018).

21. Naz, S. and Hameed, I. A., "Automated techniques for brain tumor segmentation and detection: A review study", (2017).

22. Zhang, B., "Computer vision vs. human vision", (2010).

23. Bargarai, F., Abdulazeez, A., Tiryaki, V., and Zeebaree, D., "Management of wireless communication systems using artificial intelligence-based software defined radio", (2020).

24. Zebari, D. A., Zeebaree, D. Q., Abdulazeez, A. M., Haron, H., and Hamed, H. N. A., "Improved threshold based and trainable fully automated segmentation for breast cancer boundary and pectoral muscle in mammogram images", ***Ieee Access***, 8: 203097–203116 (2020).

25. Bal, A., Banerjee, M., Sharma, P., and Maitra, M., "Brain tumor segmentation on MR image using K-Means and fuzzy-possibilistic clustering", (2018).

26. Zebari, N. A., Zebari, D. A., Zeebaree, D. Q., and Saeed, J. N., "Significant features for steganography techniques using deoxyribonucleic acid: a review", ***Indonesian Journal Of Electrical Engineering And Computer Science***, 21 (1): 338–347 (2021).

27. Preetha, R. and Jinny, S. V., "Early diagnose breast cancer with PCA-LDA based FER and neuro-fuzzy classification system", ***Journal Of Ambient Intelligence And Humanized Computing***, 12: 7195–7204 (2021).

28. Faris, M., Javid, T., Fatima, K., Azhar, M., and Kamran, R., "Detection of tumor region in MR image through fusion of Dam construction and K-mean clustering algorithms", (2019).

29. Saha, C. and Hossain, M. F., "MRI brain tumor images classification using K-means clustering, NSCT and SVM", (2017).

30. Singh, G. and Ansari, M. A., "Efficient detection of brain tumor from MRIs using K-means segmentation and normalized histogram", (2016).

31. Parmar, S. and Gondaliya, N., "A Survey on Detection and Classification of Brain Tumor from MRI Brain Images using Image Processing Techniques", (2018).

32. Joseph, R. P., Singh, C. S., and Manikandan, M., "Brain tumor MRI image segmentation and detection in image processing", ***International Journal Of Research In Engineering And Technology***, 3 (1): 1–5 (2014).

33. Havaei, M., Larochelle, H., Poulin, P., and Jodoin, P.-M., "Within-brain classification for brain tumor segmentation", ***International Journal Of Computer Assisted Radiology And Surgery***, 11: 777–788 (2016).

34. Viola, P. and Wells, W. M., "Alignment by maximization of mutual information", (1995).

35. Jahwar, A. F. and Abdulazeez, A. M., "Meta-heuristic algorithms for K-means clustering: A review", ***PalArch's Journal Of Archaeology Of Egypt/Egyptology***, 17 (7): 12002–12020 (2020).

36. Wibowo, V. V. P., Rustam, Z., and Pandelaki, J., "Classification of Brain Tumor Using K-Nearest Neighbor-Genetic Algorithm and Support Vector Machine-Genetic Algorithm Methods", (2021).

37. Modgil, S. and Kaur, B., "Lung Cancer Detection Using CT Images and Various Image Processing Techniques: A", (2019).

38. Mohan, G. and Subashini, M. M., "MRI based medical image analysis: Survey on brain tumor grade classification", ***Biomedical Signal Processing And Control***, 39: 139–161 (2018).

39. Singh, M., Garg, V., and Bhat, P., "Early Detection of Stroke using Texture Analysis", ***Indian Journal Of Forensic Medicine & Toxicology***, 13: 49–52 (2019).

40. Zhang, C., Shen, X., Cheng, H., and Qian, Q., "Brain tumor segmentation based on hybrid clustering and morphological operations", ***International Journal Of Biomedical Imaging***, 2019: (2019).

41. Al Mahmud, M. A., Karim, A. H. M. Z., Miah, M. S., Kim, Y., Kim, J., and Bashar, S. S., "Biomedical Image Processing: Spine Tumor Detection from MRI image using MATLAB", ***The Journal Of Contents Computing***, 2 (2): 225–235 (2020).

42. Lakshmi, V. K., FEROZ, C. A., and Merlin, J. A. J., "Automated detection and segmentation of brain tumor using genetic algorithm", (2018).

43. Vaidyanathan, M., Velthuizen, R., Clarke, L. P., and Hall, L. O., "Quantitation of brain tumor in MRI for treatment planning", (1994).

44. Tahir, M. N., "Classification and characterization of brain tumor MRI by using gray scaled segmentation and DNN", (2018).

45. Werring, D. J., Frazer, D. W., Coward, L. J., Losseff, N. A., Watt, H., Cipolotti, L., Brown, M. M., and Jäger, H. R., "Cognitive dysfunction in patients with cerebral microbleeds on T2*-weighted gradient-echo MRI", ***Brain***, 127 (10): 2265–2275 (2004).

46. Silfina, R. O., Indrati, R., and Utami, L. R. W., "The role T1-weighted fluid attenuated inversion recovery (FLAIR) post contrast enhancement to improve image quality on MRI brain", (2021).

47. Choi, P. K., Chung, J. Y., Lee, S. J., and Kang, H. G., "Recurrent cerebral microbleeds with acute stroke symptoms: a case report", ***Medicine***, 97 (39): (2018).

48. Tahir, B., Iqbal, S., Usman Ghani Khan, M., Saba, T., Mehmood, Z., Anjum, A., and Mahmood, T., "Feature enhancement framework for brain tumor segmentation and classification", ***Microscopy Research And Technique***, 82 (6): 803–811 (2019).

49. Rajinikanth, V. and Satapathy, S. C., "Segmentation of ischemic stroke lesion in brain MRI based on social group optimization and Fuzzy-Tsallis entropy", ***Arabian Journal For Science And Engineering***, 43 (8): 4365–4378 (2018).

50. Van Truong, P. and Thao, T. T., "Brain tumor segmentation based on U-Net with image driven level set loss", ***Vietnam Journal Of Science And Technology***, 59 (5): 634–642 (2021).

51. Akbar, S., Nasim, S., Wasi, S., and Zafar, S. M. U., "Image analysis for MRI based brain tumor detection", (2019).

52. Tjahyaningtijas, H. P. A., "Brain tumor image segmentation in MRI image", (2018).

53. Kalaiselvi, T. and Karthigai Selvi, S., "Investigation of Image Processing Techniques in MRI Based Medical Image Analysis Methods and Validation Metrics for Brain Tumor", ***Current Medical Imaging***, 14 (4): 489–505 (2018).

54. Yepuganti, K., Saladi, S., and Narasimhulu, C. V, "Segmentation of tumor using PCA based modified fuzzy C means algorithms on MR brain images", ***International Journal Of Imaging Systems And Technology***, 30 (4): 1337–1345 (2020).

55. Thamaraichelvi, B., "Modified fuzzy clustering-based segmentation through histogram combined with K-NN classification", ***International Journal Of Medical Engineering And Informatics***, 13 (5): 410–418 (2021).

56. Das, K. and Das, A., "Segmentation of Brain Tumor Using Cluster Validity Index-Based Fuzzy C-Means Algorithm", (2021).

57. Latif, G., Alghazo, J., Sibai, F. N., Iskandar, D. N. F. A., and Khan, A. H., "Recent Advancements in Fuzzy C-means Based Techniques for Brain MRI Segmentation", ***Current Medical Imaging Formerly Current Medical Imaging Reviews***, 17 (8): 917–930 (2021).

58. Biswas, B., Soroardi, H. S., and Islam, M. J., "Brain tumor detection with tumor region analysis using adaptive thresholding and morphological operation", (2018).

59. Mohammed, E., Hassaan, M., Amin, S., and Ebied, H. M., "Brain tumor segmentation: a comparative analysis", (2021).

60. Sujan, M., Alam, N., Noman, S. A., and Islam, M. J., "A segmentation based automated system for brain tumor detection", ***International Journal Of Computer Applications***, 153 (10): 41–49 (2016).

61. Tomakova, R. A., Filist, S. A., Pykhtin, A. I., and Ostrotskaia, S. V, "Classification of multichannel images based on cellular processes", ***International Multidisciplinary Scientific GeoConference: SGEM***, 19 (2.1): 145–152 (2019).

62. Cheng, J., Huang, W., Cao, S., Yang, R., Yang, W., Yun, Z., Wang, Z., and Feng, Q., "Enhanced performance of brain tumor classification via tumor region augmentation and partition", ***PloS One***, 10 (10): e0140381 (2015).

63. Brownlee, J., "Overfitting and underfitting with machine learning algorithms", ***Machine Learning Mastery***, 21: 575 (2016).

64. He, K., Zhang, X., Ren, S., and Sun, J., "Deep residual learning for image recognition", (2016).

65. Gawande, S. S. and Mendre, V., "Brain tumor diagnosis using image

processing: A survey", (2017).

66. Islam, M. K., Ali, M. S., Das, A. A., Duranta, D., and Alam, M., "Human brain tumor detection using k-means segmentation and improved support vector machine", ***International Journal Of Scientific Engineering Research***, 11 (6): 6 (2020).

67. Nasor, M. and Obaid, W., "Detection and localization of early-stage multiple brain tumors using a hybrid technique of patch-based processing, k-means clustering and object counting", ***International Journal Of Biomedical Imaging***, 2020: (2020).

68. Mehidi, I., Belkhiat, D. E. C., and Jabri, D., "An improved clustering method based on K-means algorithm for MRI brain tumor segmentation", (2019).

69. Nitta, G. R., Sravani, T., Nitta, S., and Muthu, B., "Dominant gray level based K-means algorithm for MRI images", ***Health And Technology***, 10 (1): 281–287 (2020).

70. Agrawal, R., Sharma, M., and Singh, B. K., "Segmentation of brain lesions in MRI and CT scan images: a hybrid approach using k-means clustering and image morphology", ***Journal Of The Institution Of Engineers (India): Series B***, 99: 173–180 (2018).

71. ShanmugaPriya, S. and Valarmathi, A., "Efficient fuzzy c-means based multilevel image segmentation for brain tumor detection in MR images", ***Design Automation For Embedded Systems***, 22: 81–93 (2018).

72. Zotin, A., Simonov, K., Kurako, M., Hamad, Y., and Kirillova, S., "Edge detection in MRI brain tumor images based on fuzzy C-means clustering", ***Procedia Computer Science***, 126: 1261–1270 (2018).

73. Sheela, C. J. J. and Suganthi, G., "Morphological edge detection and brain tumor segmentation in Magnetic Resonance (MR) images based on region growing and performance evaluation of modified Fuzzy C-Means (FCM) algorithm", ***Multimedia Tools And Applications***, 79: 17483–17496 (2020).

74. Yepuganti, K., Saladi, S., and Narasimhulu, C. V., "Segmentation of tumor using PCA based modified fuzzy C means algorithms on MR brain images", ***International Journal Of Imaging Systems And Technology***, 30 (4): 1337–1345 (2020).

75. Alam, M. S., Rahman, M. M., Hossain, M. A., Islam, M. K., Ahmed, K. M., Ahmed, K. T., Singh, B. C., and Miah, M. S., "Automatic human brain tumor detection in MRI image using template-based K means and improved fuzzy C means clustering algorithm", ***Big Data And Cognitive Computing***, 3 (2): 27 (2019).

76. Seetha, J. and Raja, S. S., "Brain tumor classification using convolutional neural networks", ***Biomedical & Pharmacology Journal***, 11 (3): 1457 (2018).

77. Hamad, Y., Mohammed, O. K. J., and Simonov, K., "Evaluating of tissue germination and growth rate of ROI on implants of electron scanning microscopy images", (2019).

78. Suzuki, K., "Overview of deep learning in medical imaging", ***Radiological Physics And Technology***, 10 (3): 257–273 (2017).

79. Beale, M. H., Hagan, M. T., and Demuth, H. B., "Matlab Neural network toolbox user's guide (R2012a)", ***Mathworks Inc Natick Mass Usa***, (2012).

80. Brainweb, B., "Simulated brain database", ***Online: Http://Brainweb. Bic. Mni. Mcgill. Ca/Cgi/Brainweb2.–2010***, (2010).

81. Glaser, J., Greene, G., and Hendricks, S., "Stereology for Biological Research: With a Focus on Neuroscience", ***Mbf Press***, (2007).

82. Hara, H., Hori, T., Sugahara, K., and Yamashita, H., "Surgical planning of Isshiki type I thyroplasty using an open-source Digital Imaging and Communication in Medicine viewer OsiriX", ***Acta Oto-Laryngologica***, 134 (6): 620–625 (2014).

83. Heath, M., Bowyer, K., Kopans, D., Kegelmeyer, P., Moore, R., Chang, K., and Munishkumaran, S., "Current status of the digital database for screening mammography", ***Digital Mammography: Nijmegen, 1998***, 457–460 (1998).

84. Mohanty, F., Rup, S., Dash, B., Majhi, B., and Swamy, M. N. S., "Digital mammogram classification using 2D-BDWT and GLCM features with FOA-based feature selection approach", ***Neural Computing And Applications***, 32: 7029–7043 (2020).

85. Wu, W., Chen, A. Y. C., Zhao, L., and Corso, J. J., "Brain tumor detection and segmentation in a CRF (conditional random fields) framework with pixel-pairwise affinity and superpixel-level features", ***International Journal Of Computer Assisted Radiology And Surgery***, 9: 241–253 (2014).

86. Xiang, Z., Tan, H., and Ye, W., "The excellent properties of a dense grid-based HOG feature on face recognition compared to Gabor and LBP", ***IEEE Access***, 6: 29306–29319 (2018).

87. Zhou, W., Gao, S., Zhang, L., and Lou, X., "Histogram of oriented gradients feature extraction from raw bayer pattern images", ***IEEE Transactions On Circuits And Systems II: Express Briefs***, 67 (5): 946–950 (2020).

88. Greeshma, K. V and Sreekumar, K., "Fashion-MNIST classification based on HOG feature descriptor using SVM", ***International Journal Of Innovative Technology And Exploring Engineering***, 8 (5): 960–962 (2019).

89. Tuncer, T., Dogan, S., and Ozyurt, F., "An automated Residual Exemplar Local Binary Pattern and iterative ReliefF based COVID-19 detection method using chest X-ray image", ***Chemometrics And Intelligent Laboratory Systems***, 203: 104054 (2020).

90. Konstantinidis, D., Stathaki, T., Argyriou, V., and Grammalidis, N., "Building detection using enhanced HOG–LBP features and region refinement processes", ***IEEE Journal Of Selected Topics In Applied Earth Observations And Remote Sensing***, 10 (3): 888–905 (2016).

91. Yang, J., Chen, Z., Zhang, J., Zhang, C., Zhou, Q., and Yang, J., "HOG and SVM algorithm based on vehicle model recognition", (2020).

92. Krishan, A. and Mittal, D., "Multi-class liver cancer diseases classification using CT images", ***The Computer Journal***, 66 (3): 525–539 (2023).

93. Hamad, Y. A., Simonov, K., and Naeem, M. B., "Brain's tumor edge detection on low contrast medical images", (2018).

94. Cheng, J., "Brain magnetic resonance imaging tumor dataset", ***Figshare MRI Dataset Version***, 5: (2017).

95. Hu, K., Gan, Q., Zhang, Y., Deng, S., Xiao, F., Huang, W., Cao, C., and Gao, X., "Brain tumor segmentation using multi-cascaded convolutional neural networks and conditional random field", ***IEEE Access***, 7: 92615–92629 (2019).

96. Chen, G., Li, Q., Shi, F., Rekik, I., and Pan, Z., "RFDCR: Automated brain lesion segmentation using cascaded random forests with dense conditional random fields", ***NeuroImage***, 211: 116620 (2020).

97. Zhang, D., Huang, G., Zhang, Q., Han, J., Han, J., Wang, Y., and Yu, Y., "Exploring task structure for brain tumor segmentation from multi-modality MR images", ***IEEE Transactions On Image Processing***, 29: 9032–9043 (2020).

98. Zhou, C., Ding, C., Wang, X., Lu, Z., and Tao, D., "One-pass multi-task networks with cross-task guided attention for brain tumor segmentation", ***IEEE Transactions On Image Processing***, 29: 4516–4529 (2020).

99. Zhang, D., Huang, G., Zhang, Q., Han, J., Han, J., and Yu, Y., "Cross-modality deep feature learning for brain tumor segmentation", ***Pattern Recognition***, 110: 107562 (2021).

RESUME

Her name is Ruaa Mashkoor MAHMOOD. Her elementary education in IRAQ. after that, she started undergraduate program in The Islamic University Department of Computer Engineering in 2018. To complete M. Sc. education, she moved to Karabük University in 2021.